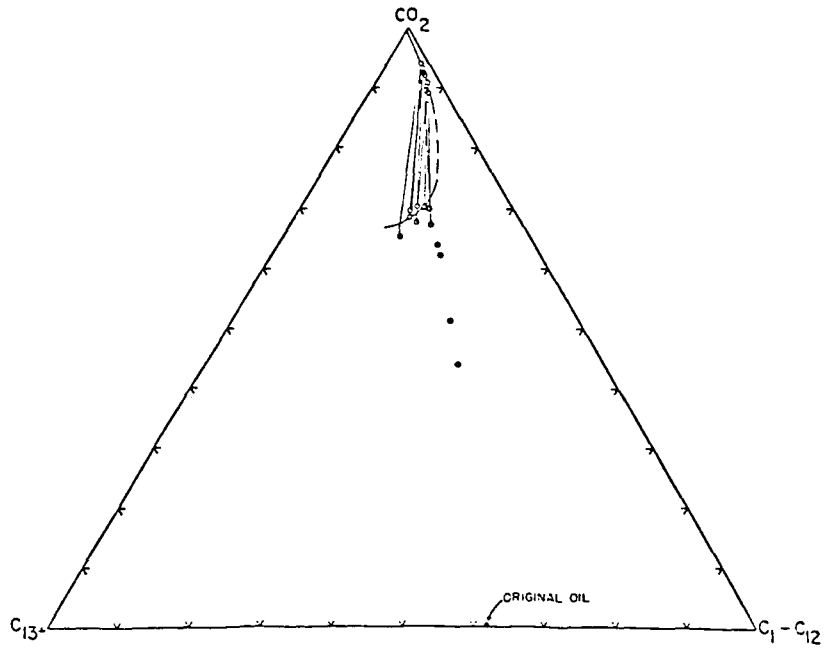

Fig. 5.3 Pseudo-ternary representation of phase compositions for mixtures of CO_2 with Maljamar separator oil at 8270 kPa and 32°C.

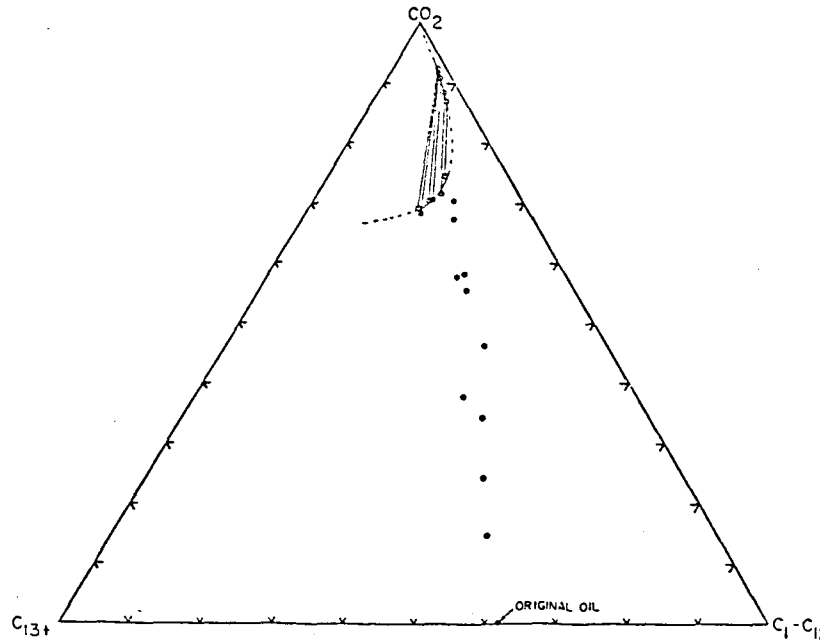

Fig. 5.4 Pseudo-ternary representation of phase compositions for mixtures of CO_2 with Maljamar separator oil at 9650 kPa and 32°C.

At 6890 kPa (Fig. 5.2), the phase diagram is much more complex. The displacement entered the liquid-liquid (L_1-L_2) region first and then with continued CO_2 injection reached the liquid-liquid-vapor (L_1-L_2-V) region. The tie lines shown in the L_1-L_2 region confirm that more efficient extraction of C_1-C_{12} hydrocarbons takes place in the L_1-L_2 region than in the L_1-V region. At 8270 kPa (Fig. 5.3), the displacement passed only through the liquid-liquid region in which extraction of hydrocarbons was much more efficient. Similar behavior was observed at 9650 kPa (Fig. 5.4). The differences between the two displacements at the higher pressures were smaller because compositions of liquid-liquid systems are much less sensitive to pressure changes than are those of liquid-vapor systems.

Gas-oil relative permeability data given by Naar, Wygal, and Henderson (1962) for unconsolidated sands were used without adjustment. Because the experimentally determined phase diagrams reported here match closely those proposed by Orr, Yu, and Lien (1981) based on single contact PVT data and an analysis of the behavior of binary and ternary CO_2-hydrocarbon systems, their discussion of simulation of the effects of phase behavior on displacement efficiency also applies here and will not be repeated.

Component properties used in the simulations of the slim tube displacements are given in Table 5.1. The viscosities shown in Table 5.1 were interpolated from data of Michels, Botzen, and Schuurman (1957). The viscosities and densities of the hydrocarbon pseudo-components were estimated (McCain 1973) so that the overall density and viscosity of the oil matched measured values. Hydrocarbon component densities were assumed to be the same in all phases. The density of CO_2 in a vapor phase was taken to be that of pure CO_2. The apparent density of CO_2 in liquid phases, however, was calculated from densities measured in the continuous multiple contact experiment. For simulations of the displacements at 8270 and 9650 kPa, slightly different apparent CO_2 densities in the CO_2-rich liquid were used in different regions of the phase diagram to reflect the experimental observation that the apparent density of CO_2 is not constant over large ranges in composition (Orr, Silva & Lien 1983). The two values used are also given in Table 5.1.

Slim tube studies were performed using a 12.2 m (40 ft.), 0.635 cm (1/4 in.) ID stainless steel tube packed with 170-200 mesh glass beads. The slim tube had a pore volume of 147.3 cm^3 and a permeability of 5800 md. The packed tube was rolled into a 25.4 cm (10 in.) diameter coil and installed in a temperature controlled water bath. In all slim tube displacements, the bead pack was first completely saturated with oil, then CO_2 was injected into the top, and fluids were produced from the bottom of the coiled tube. Just prior to the start of CO_2 injection, oil was displaced through the pack at the run displacement rate to establish a pressure gradient, with the pressure at the outlet controlled to the test pressure by a back pressure regulator. Then, CO_2 injection was started at the same rate. The amount of oil recovered was determined by weight rather than by less accurate volumetric measurements.

Results of displacements at the same conditions as those used in the continuous multiple contact experiments are given in Fig. 5.5. The scales used to plot Fig. 5.5 deserve some comment. The time scale is presented as

Table 5.1 Component Properties for Simulations of Slim Tube Displacements

Component	Molecular Weight	Viscosity (mPa·s)			
		5520 kPa	6890 kPa	8270 kPa	9650 kPa
CO_2	44	0.0176	0.021	0.052	
C_5-C_{12}	119	0.89	0.89	0.89	0.89
C_{13+}	323	18.96	18.96	18.96	18.96

Component	Density (g/cm^3)								
	5520 kPa		6890 kPa			8270 kPa		9650 kPa	
	Vapor	Liquid	Vapor	CO_2-rich Liquid	Oil-rich Liquid	CO_2-rich Liquid	Oil-rich Liquid	CO_2-rich Liquid	Oil-rich Liquid
CO_2	0.143	0.918	0.2313	0.780	0.898	0.74, 0.82	0.895	0.79, 0.83	0.893
C_5-C_{12}	0.689	0.689	0.696	0.696	0.696	0.702	0.702	0.708	0.708
C_{13+}	0.978	0.978	0.978	0.978	0.978	0.978	0.978	0.978	0.978

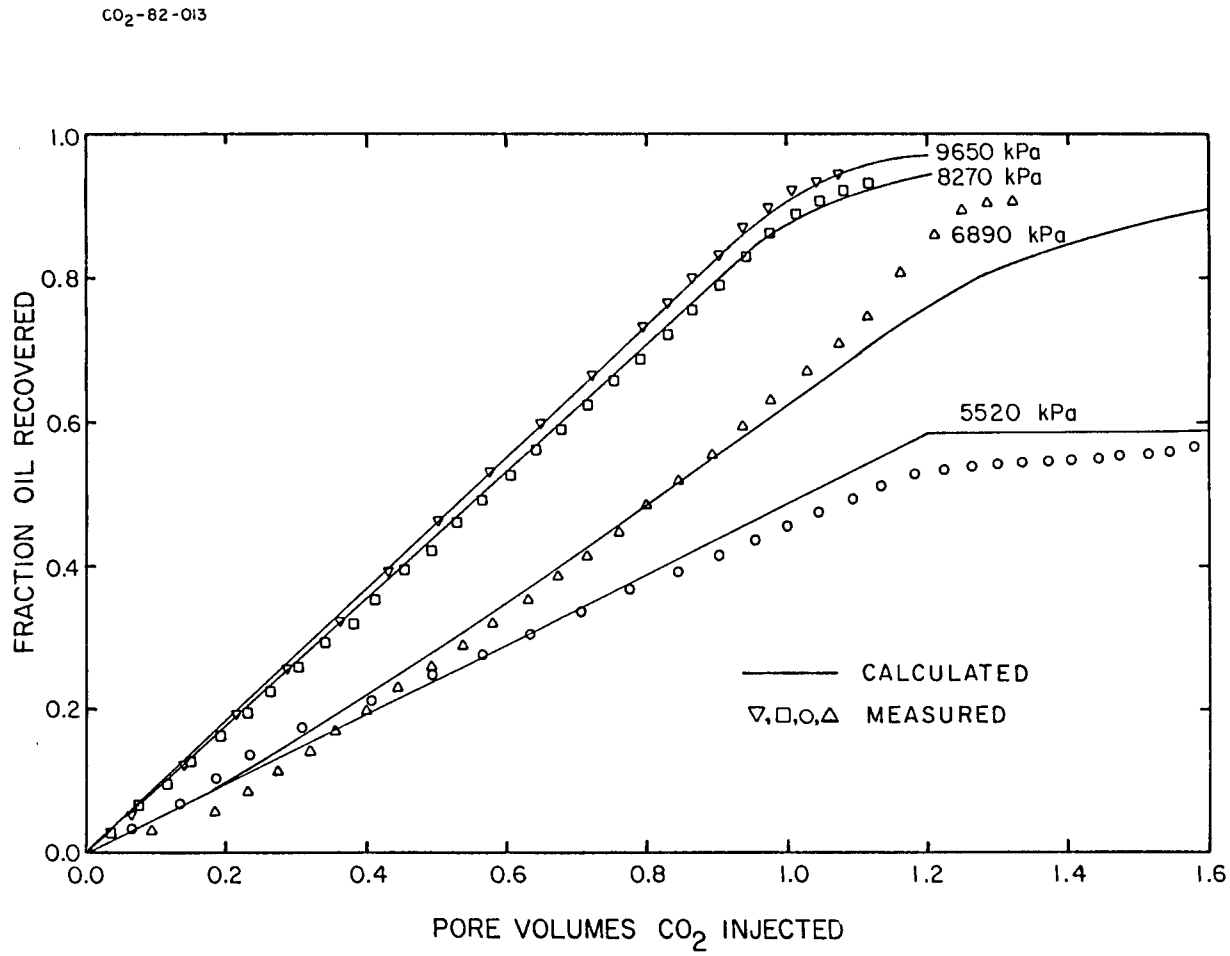

Fig. 5.5 Comparison of calculated (line) and experimental (symbols) oil recovery in slim tube displacements of Maljamar separator oil by CO_2 at 32°C.

pore volumes of CO_2 injected. Because the run temperature was very near the critical temperature of CO_2, its density was sensitive to the change in pressure gradient which occurred as low viscosity CO_2 replaced high viscosity oil. The volume of CO_2 injected at a point during the run was calculated as the volume of mercury injected into the thermostatted CO_2 supply vessel plus the expansion of the total volume of CO_2.

It is clear from Fig. 5.5 that the volume of CO_2 calculated as described above is not an accurate measure of the actual volume of oil displaced at 5520 and 6890 kPa (800 and 1000 psia). In those displacements, the amount of oil recovered early in the runs was significantly less than the apparent volume injected, and in both runs CO_2 breakthrough occurred at an apparent injection of more than one pore volume. The explanation for the observed behavior lies in the interplay of the solubility of CO_2 in the oil, volume change on mixing, and the effect of component partitioning on displacement efficiency. In the displacement at 5520 kPa, very little extraction of hydrocarbons by CO_2 occurred (Fig. 5.1). Consequently, the displacement was immiscible, the local displacement efficiency was low, and almost 50 percent of the oil was left behind at CO_2 breakthrough. That oil was saturated with CO_2, however, and since the quantity of oil left behind was large, the amount of CO_2 required to saturate it was also large. The apparent density of CO_2 dissolved in the oil (defined as the mass of CO_2 dissolved divided by the volume increase of the swollen oil over original oil) is, however, much greater than the density of pure CO_2 at the same pressure. Thus, the effect of the volume change of CO_2 upon dissolution in the oil is to reduce the effective volume of CO_2 injected.

The displacements at 8270 and 9650 kPa (1200 and 1400 psia) were affected much less by volume change on mixing for two reasons. First, the density of pure CO_2 was much nearer the apparent density of CO_2 in solution, so that there was much less volume change. Second, the local displacement efficiency was much higher, and hence there was much less oil remaining to be saturated with CO_2. Thus, the corrections for volume change were much smaller at the higher pressures. Simulation results reported below confirm this explanation.

It is evident from the results shown in Fig. 5.5 that the displacement of oil by vapor phase CO_2 at 5520 kPa was much less efficient than the displacements in which a CO_2-rich liquid phase was present. The phase compositions presented above clearly indicate that extraction of hydrocarbons by a CO_2-rich liquid is more efficient than that of a vapor, but that fact alone does not prove that more efficient extraction is responsible for the dramatic improvement in oil recovery at 6890 kPa over that obtained at 5520 kPa. The solubility of CO_2 in the oil changes with pressure as does its viscosity and density. Assessment of the relative importance of variations of extraction, solubility and fluid properties is a task for simulation.

Fig. 5.5 also compares calculated oil recoveries with the experimental results. With the exception of the run at 6890 kPa, the agreement is good. Calculated oil recoveries increase with increasing pressure, and the rates of recovery in the simulated displacements match well with the experimental rates. Fig. 5.6 shows computed saturation distributions for each displacement at 0.8 PV injected (based on the density of pure CO_2 at the displacement pressure). At 5520 kPa, the liquid phase occupies more than 50% of the volume

of the swept zone though part of that volume is dissolved CO_2. Also plotted in Fig. 5.6 is the ratio of the mole fraction of the light hydrocarbon pseudo-component (C_5-C_{12}) to that of the heavy hydrocarbon pseudo-component (C_{13+}). Because the vapor phase at 5520 kPa extracts only small quantities of hydrocarbons, the ratio hardly changes. The only compositional effect in that displacement comes from the solubility of the CO_2 in the oil. Because the displacement is relatively inefficient and the solubility and apparent density of CO_2 are both high, much of the injected CO_2 simply dissolves in the oil rather than displacing it. Thus, the displacement proceeds slowly as shown in Fig. 5.5.

At 6890 kPa, a CO_2-rich liquid (L_2) displaces oil and is in turn displaced by CO_2-rich vapor. The residual liquid phase is much smaller, and the ratio of light to heavy hydrocarbons indicates a zone in which the L_2 phase has preferentially extracted light hydrocarbons. Because the residual oil phase is smaller and because the injected CO_2 is denser, there is less volume change and the displacement proceeds more rapidly on a time scale based on the volume of pure CO_2 injected. At 8270 kPa, the displacement is still more efficient. The saturation of the residual L_1 phase is smaller, and the ratio of light to heavy hydrocarbons indicates more efficient extraction. At 9650 kPa, the transition zone enriched in light hydrocarbons is sharper and the residual saturation is slightly smaller than at 8270 kPa. Both displacements recover well over 90% of the oil in place (Fig. 5.5).

The difference between the computed and observed recovery at 6890 kPa deserves comment. The total amount of oil recovered in the simulation is nearly the same as that observed, but the time scale in the simulation is obviously not correct late in the run. This occurs because the representation of phase densities in the simulator is too simple. Measurements at 6890 kPa (Orr, Jensen & Silva 1981) suggest that the density of the CO_2-rich liquid declines rapidly as the overall composition approaches the liquid-liquid-vapor region. That fact is not modeled in the simulator, which treats the density of CO_2 in the CO_2-rich liquid as constant. Therefore, late in the calculated displacement, the CO_2 present in the CO_2-rich liquid occupies less volume than in the experiment, and hence the calculated rate of fluid production is too low.

As Fig. 5.5 indicates, recovery of oil in slim tube displacements increases with increasing pressure, as has long been known. Even in a very simple porous medium, however, displacement of oil by CO_2 is the result of a complex interplay of phase behavior, fluid properties and multiphase flow. Sensitivity studies with the simulator used here, as well as with the version which does not allow volume change on mixing, lead to the following observations:

(1) The viscosity of CO_2, or of a CO_2-rich phase, is sufficiently low that the increase in that viscosity with pressure produces a negligible increase in oil recovery if all other factors are held constant. The efficiency of such adverse mobility displacements remains low. Thus, changes in the viscosity of CO_2 do not account for improved recovery with increasing pressure.

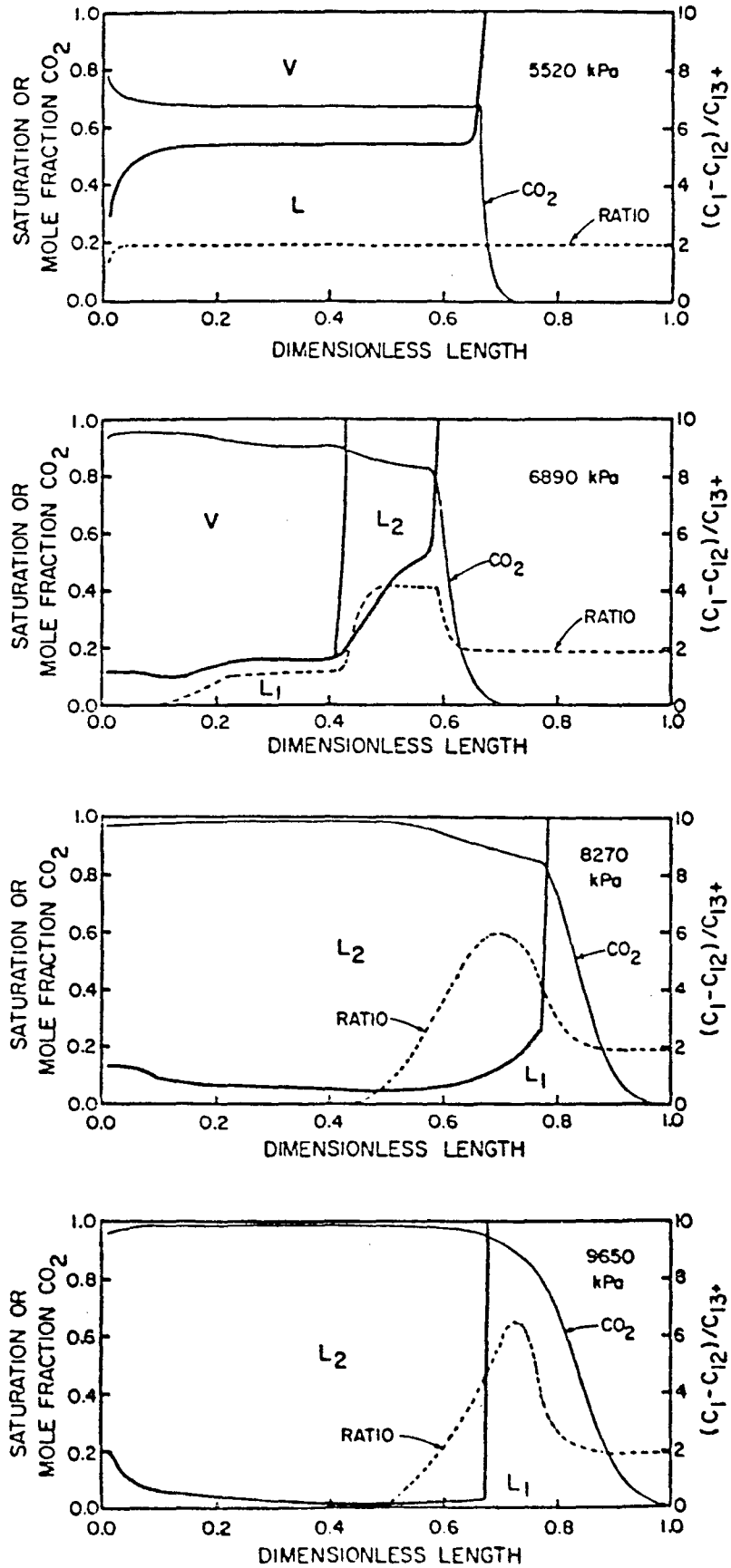

Fig. 5.6 Calculated saturation and composition profiles at 0.8 pore volumes CO_2 injected.

(2) An increase in the density of dissolved CO_2, with other factors constant, reduces oil recovery because the volume occupied by CO_2 in the oil phase is lower.

(3) An increase in the solubility of CO_2 in oil increases recovery because the fraction of the remaining oil phase which is actually oil is reduced. However, the solubility of CO_2 in crude oil usually does not exceed 60-80 mol % at reasonable pressures and typical CO_2 volume fraction at such pressures would be less than 0.50. Thus, solubility increases alone do not explain recoveries of 95%.

(4) Improvement in the efficiency with which CO_2 extracts light and intermediate hydrocarbons from the oil, with all other factors constant, does produce an increase in recovery. Simulations presented here and by Gardner, Orr, and Patel (1981) and Orr, Yu, and Lien (1981) clearly establish that improved extraction can account for improved recovery with increasing pressure in CO_2-crude oil systems in which the temperature is low enough that liquid-liquid phase behavior occurs.

(5) Total recovery is determined by phase behavior, but the rate of recovery is determined by volume change on mixing.

The combination of simulations and experiments presented offers some guidance on the selection of pressure levels for field projects. Because extraction by a dense CO_2-rich liquid phase is so much more efficient than that of a low density vapor phase, and because extraction (or vaporization in systems too high in temperature to show liquid-liquid behavior) accounts for the high local displacement efficiency which is a fundamental part of any successful CO_2 flood, it seems reasonable to select an operating pressure which avoids the presence of a phase of high mobility and low extractive power. The simple correlation discussed in §3 can be used to estimate that pressure. It has been suggested, however, that it might be beneficial to operate a CO_2 flood in the liquid-liquid-vapor region to take advantage of the mobility control which might result from the interference to flow of multiple phases (Henry & Metcalfe 1980; Yellig 1982). In any case, the pressure ranges over which three phases coexist are fairly small, so that controlling field pressure to stay within that range in a significant fraction of a reservoir might be difficult. We believe that it would be preferable to err on the high-pressure side of the liquid-liquid-vapor region where extraction is known to be more efficient.

The simulator used here is, by design, simple in its mathematical approach and in the representation of the complex phase behavior of CO_2-crude oil systems. Nevertheless, it produces results which agree well with experimental displacements. Given the simplicity of the representations used for the phase behavior and density effects, the agreement obtained is remarkable. We emphasize that no attempt was made to adjust the phase behavior, fluid properties, or relative permeabilities used in the simulations. The calculated oil recoveries are, therefore, predictions based

solely on independent measurements of phase compositions and densities for the CO_2-crude oil system used. The fact that good quantitative agreement was obtained between prediction and experiment offers encouragement that representations of CO_2-crude oil phase behavior in terms of a small number of pseudo-components may be feasible. Such representations are essential if field-scale simulations which account for phase behavior are to be successful.

5.2 Effects of Trapped and Dendritic Saturations: Model Formulation and Validation

In the simulations discussed in §5.1 the porous medium was assumed to be uniform and fluids were taken as locally well mixed, reasonable assumptions for flow in a slim tube. As the review of §4.1 and the experimental results presented in §4.4 indicate, that assumption may not be reasonable for some reservoir rocks in which the pore space is heterogeneous at the microscopic level. In addition, the presence of high water saturations may lead to the isolation of some oil by water and to oil given the shape of dead-end or dendritic ganglia by surrounding water, as the flow visualizations of §3.3 clearly indicated (see Fig. 3.12, for instance). In this section we describe a model designed to allow an assessment of the impact of alterations to mixing due to microscopic heterogeneity, or high water saturations, when effects of phase behavior are also important. Because the model is one-dimensional, effects of viscous instability are not modeled.

Assumptions

The model described here is based on the following assumptions in addition to those outlined in §4.1:

(1) The portion of pore space occupied by nonwetting phase(s) is divided into flowing, dendritic and trapped fractions, which depend only on the water saturation.

(2) Fluid in the dendritic fraction exchanges material with fluid in the flowing fraction by mass transfer assumed to be proportional to the difference in overall composition between the two fractions.

(3) Fluid in the trapped fraction has uniform composition and is isolated from other fractions. Its composition changes only if the trapped fraction changes due to a change in the water saturation.

(4) If the flowing fraction decreases during a time step, fluid of the overall composition of the flowing fraction is transferred first to the dendritic fraction, with any excess transferred to the trapped fraction. If the flowing fraction increases, fluid is released first from the dendritic fraction.

(5) If the trapped fraction increases, fluid having the overall composition is transferred first from the dendritic fraction. If it decreases, fluid is released first to the dendritic fraction.

(6) Volume change on mixing in the trapped fraction is ignored. If the volume of fluid in the dendritic fraction shrinks after mixing, additional fluid is moved from the flowing fraction during the next time step to make up the lost volume. The flow rate out of the grid block is adjusted to account for volume change on mixing in both the dendritic and flowing fractions.

Assumption (1) is the same as that used by Salter and Mohanty (1982) in the analysis of their two-phase displacements. It is equivalent to the division of the pore space envisioned in the Coats-Smith model with the addition of an isolated fraction. Assumption (2) is also equivalent to the formulation of the Coats-Smith model, although it includes the additional assumption that a single mass transfer coefficient can be used to model the transfer between the dendritic and flowing fractions. While more complex models using different mass transfer coefficients in each phase, for instance, could be formulated, experimental data required to support such models are simply not available. Hence, only use of the simplest description of mass transfer seems justified at this stage.

Assumption (3) contains two idealizations not strictly in accord with probable behavior of fluids in real displacements. First, fluid in the trapped fraction is assumed to be completely mixed, even though fluids trapped at different times have different compositions. Fluids which become trapped during flow in a real porous medium probably remain physically segregated. Unfortunately, a calculation which rigorously accounted for the compositions of fluids trapped at different times and, for instance, released first fluid that was trapped last, would require a set of compositions to be stored for each time step during which the trapped fraction increased. The computer storage required would be unacceptably large even for a one-dimensional calculation. Hence, the assumption of uniform composition in the trapped phase is based on computational necessity. The second part of assumption (3), that trapped fluid is completely isolated, ignores the diffusion of CO_2 through water. As was demonstrated in §3.4, CO_2 can diffuse through water to reach trapped oil. Examination of the effects of that transport of CO_2 awaits experimental determination of diffusion rates along the lines suggested in §3.4.

Assumptions (4) and (5) are made because there must be some recipe for the transfer of fluids as the flowing, dendritic and trapped fractions change with the water saturation. It seems physically plausible that fluid in the dendritic fraction would be the first to be trapped by a rising water saturation and that fluid released from the trapped fraction would be dendritic, but there is only the experimental evidence of the flow visualizations of §3.3 in support of the assumption. In the absence of experimental evidence to the contrary, the assumptions appear as reasonable as others we considered.

The final assumption is consistent with the explicit calculation scheme used to solve the material balance equations developed based on the first five assumptions. Neglect of volume change in the trapped fraction seems justified by the fact that trapped fluids are probably physically segregated.

Material Balance Equations

A material balance for the water phase yields

$$\frac{\partial S_w}{\partial \tau} + \frac{\partial}{\partial \xi}\left(F_w \frac{q}{q_i}\right) = 0 \tag{5.5}$$

For each component in the nonwetting phase, a balance on moles of component i in the flowing fraction gives

$$\frac{\partial}{\partial \tau}\sum_{j=1}^{n_p} f_f\, x_{ij}^f\, \rho_j^f\, S_j^f + \frac{\partial}{\partial \xi}\sum_{j=1}^{n_p} x_{ij}^f\, \rho_j^f\, F_j\, \frac{q}{q_i} + \frac{\partial}{\partial \tau}\sum_{j=1}^{n_p}\left(f_d\, x_{ij}^d\, \rho_j^d\, S_j^d + f_t\, x_{ij}^t\, \rho_j^t\, S_j^t\right) = 0 \qquad i = 1, n_c \tag{5.6}$$

and balances for the dendritic and trapped fractions yield

$$\frac{\partial}{\partial \tau}\sum_{j=1}^{n_p} f_d\, x_{ij}^d\, \rho_j^d\, S_j^d = \left(R_{2i} - R_{1i}\right)\frac{AL}{q_i} \qquad i = 1, n_c \tag{5.7}$$

and

$$\frac{\partial}{\partial \tau}\sum_{j=1}^{n_p} f_t\, x_{ij}^t\, \rho_j^t\, S_j^t = -\left(R_{2i} + R_{3i}\right)\frac{AL}{q_i} \qquad i = 1, n_c \tag{5.8}$$

where

R_{1i} = rate of transfer of component i per unit volume of moles from the dendritic to the flowing fraction.

R_{2i} = rate of transfer of component i per unit volume from the trapped to the dendritic fraction.

R_{3i} = rate of transfer of component i per unit volume from the trapped to the flowing fraction.

In addition, the following conditions hold

$$f_f + f_d + f_t = 1 \tag{5.9}$$

$$\sum_{j=1}^{n_p} S_j^{\alpha} = 1 \qquad \alpha = f, d, t \tag{5.10}$$

$$\sum_{i=1}^{n_c} x_{ij} = 1 \qquad j = 1, n_p \tag{5.11}$$

The rate terms of eqs. (5.7) and (5.8) are specified according to assumptions (2)-(5). The composition of fluid in the trapped fraction changes only if the trapped fraction itself changes due to a change in the water saturation. Thus, by assumption (5), R_{2i} is given by

$$R_{2i} = -\phi \rho^* x_i^* \frac{\partial f_t}{\partial \tau} \left(\frac{q_i}{AL}\right) \tag{5.12}$$

where $\rho^* x_i^*$ is the average concentration of component i in the fraction from which the transfer is made. Thus, if the trapped fraction increases, $\partial f_t/\partial \tau > 0$ and

$$\rho^* x_i^* = \sum_{j=1}^{n_p} x_{ij}^d \rho_j^d S_j^d \tag{5.13}$$

If the trapped fraction is decreasing, $\partial f_t/\partial \tau < 0$ and

$$\rho^* x_i^* = \sum_{j=1}^{n_p} x_{ij}^t \rho_j^t S_j^t \tag{5.14}$$

In simulations where water saturations are changing rapidly, it sometimes happens that the change in the trapped fraction is greater than the dendritic fraction. In such cases, the excess material is transferred to or from the flowing fraction. Only in this case is R_{3i} different from zero. For example, if the increase in f_t over a time step $\Delta\tau$, Δf_t, exceeds the dendritic fraction f_d, then

$$R_{2i}\,\Delta\tau = -\rho^{d}\,x_i^{d}\,f_d\left(\frac{q_i}{AL}\right)$$

and (5.15)

$$R_{3i}\,\Delta\tau = -\rho^{f}\,x_i^{f}\left(\Delta f_t - f_d\right)\left(\frac{q_i}{AL}\right)$$

The transfer rate from the dendritic to the flowing fraction includes contributions from mass transfer and changes in the various fractions. By assumption (2), the rate of mass transfer has the form

$$-K\left(\rho^{f}x_i^{f} - \rho^{d}x_i^{d}\right)$$

where

$$\rho^{f}\,x_i^{f} = \sum_{j=1}^{n_p} x_{ij}^{f}\,\rho_j^{f}\,S_j^{f} \qquad (5.16)$$

and

$$\rho^{d}\,x_i^{d} = \sum_{j=1}^{n_p} x_{ij}^{d}\,\rho_j^{d}\,S_j^{d}$$

The rate of transfer of material from the dendritic to the flowing fraction due to a change in the water saturation is given by

$$\rho^{o}\,x_i^{o}\,\frac{\partial f_f}{\partial\tau}\left(\frac{q_i}{AL}\right)$$

where

$$\rho^{o}\,x_i^{o} = \sum_{j=1}^{n_p} x_{ij}^{f}\,\rho_j^{f}\,S_j^{f} \qquad (5.17)$$

if $\frac{\partial f_f}{\partial\tau} < 0$ and

$$\rho^{o}\,x_i^{o} = \sum_{j=1}^{n_p} x_{ij}^{d}\,\rho_j^{d}\,S_j^{d}$$

if $\frac{\partial f_f}{\partial \tau} > 0$.

Thus, the overall rate of transfer from the dendritic to the flowing fraction is

$$R_{li} = -K\left(\rho^f x_i^f - \rho^d x_i^d\right) + \rho^o x_i^o \frac{\partial f_f}{\partial \tau}\left(\frac{q_i}{AL}\right) \tag{5.18}$$

The final relationship needed for calculation of relative permeabilities is

$$S_j = \sum_\alpha S_j^\alpha f_\alpha \tag{5.19}$$

Eq. (5.19) simply states that the total saturation of a phase is the sum of the saturations in the various fractions.

Eqs. (5.5)-(5.8) along with the definitions of eqs. (5.9)-(5.18) were solved with a fully explicit finite difference representation similar to that described in §5.1. As in §5.1, numerical dispersion was used to represent physical dispersion. If flowing and dendritic fractions are fixed, only one phase is present and there is no volume change on mixing, then eqs. (5.5)-(5.8) reduce to eq. (4.8). Thus, the analysis of numerical dispersion of §4.3 applies. For the more general case of variable flowing, dendritic and trapped fractions and multiphase flow, the numerical representation of dispersion is only qualitative.

The algorithm used to solve eqs. (5.5)-(5.8) was, therefore

(1) Use eq. (5.5) to calculate new water saturations.

(2) Calculate component transfer rates due to changes in the trapped and dendritic fractions resulting from changes in the water saturation and due to mass transfer to or from the dendritic fraction using eqs. (5.12)-(5.18).

(3) Calculate rate of transfer of material from the flowing to the dendritic fraction to make up any volume change on mixing during the previous time step.

(4) Perform flash calculations to determine phase compositions in the trapped, dendritic and flowing fractions. Calculate phase saturations, densities, viscosities, relative permeabilities and fractional flows.

(5) Adjust local flow rate to account for volume change on mixing in both the flowing and dendritic fractions.

(6) Use the material balance eqs. (5.6)-(5.8) to calculate new overall compositions in the flowing, dendritic and trapped fractions.

(7) Return to (1).

Model Validation

To test the operation of the new version of the simulator, simulations of the displacements described in §5.1 were repeated, with the flowing fraction set to one. Results of the previous calculations were duplicated by the new version. Simulations for the flow of one phase with fixed flowing and dendritic fractions and no trapped fraction were also performed. In such cases, the simulator simply solves the Coats-Smith model. Figs. 5.7 and 5.8 compare solutions for effluent compositions obtained with the simulator with solutions reported by Coats and Smith (1964) and Salter and Mohanty (1982) for the parameter values shown on the plots. Clearly, the new model simulates accurately displacements for which solutions are known.

5.3 Phase Behavior, Mixing and Flow: Interactions in Nonuniform Pore Structures

The displacement experiments of §4.4 indicate clearly that microscopic heterogeneity in some reservoir rocks can lead to mixing which is significantly different from that observed in slim tube displacements. Because mixing affects the compositions of fluid mixtures that occur during a displacement, alterations to mixing must affect process performance if composition path and phase behavior are important. In this section, we examine the effects of microscopic heterogeneity on the efficiency of displacements of Maljamar crude oil at 1200 psia and 90°F. Slim tube results shown in Fig. 5.5 indicate that at such conditions, the displacement is miscible in the multiple contact sense. Two sources of microscopic heterogeneity are considered. In the first, the porous medium itself is heterogeneous enough that the assumption that fluids are locally well mixed is no longer valid. The Seminole and San Andres outcrop carbonate samples described in §4.4 and §4.5 are examples. The second source of microscopic heterogeneity is the presence of water. The flow visualization experiments of §3.3 clearly indicated that high water saturations can produce dendritic oil even when there are no dead-end pores in the porous medium, as did the measurements of Salter and Mohanty (1982) for a Berea sandstone core.

Pore Structure Heterogeneity

Results of simulations of the displacement of Maljamar crude oil by CO_2 at 1200 psia and 90°F for nonuniform porous media are shown in Fig. 5.9. Results of similar simulations at other pressures are reported by Dai (1984). Shown are calculated effluent CO_2 concentrations for three values of the flowing fraction, 0.5, 0.7 and 0.9. Peclet and Damköhler numbers were held constant. Relative permeabilities used were the same as those used for the simulations of §5.1. As in the single-phase displacements, a lower flowing fraction leads to earlier breakthrough and more tailing. In actual CO_2 core floods, viscous instability would cause even earlier CO_2 breakthrough unless the displacements were gravity stabilized. Comparison of Figs. 5.8 and 5.9 indicates that CO_2 concentrations rose more rapidly than did injected fluid

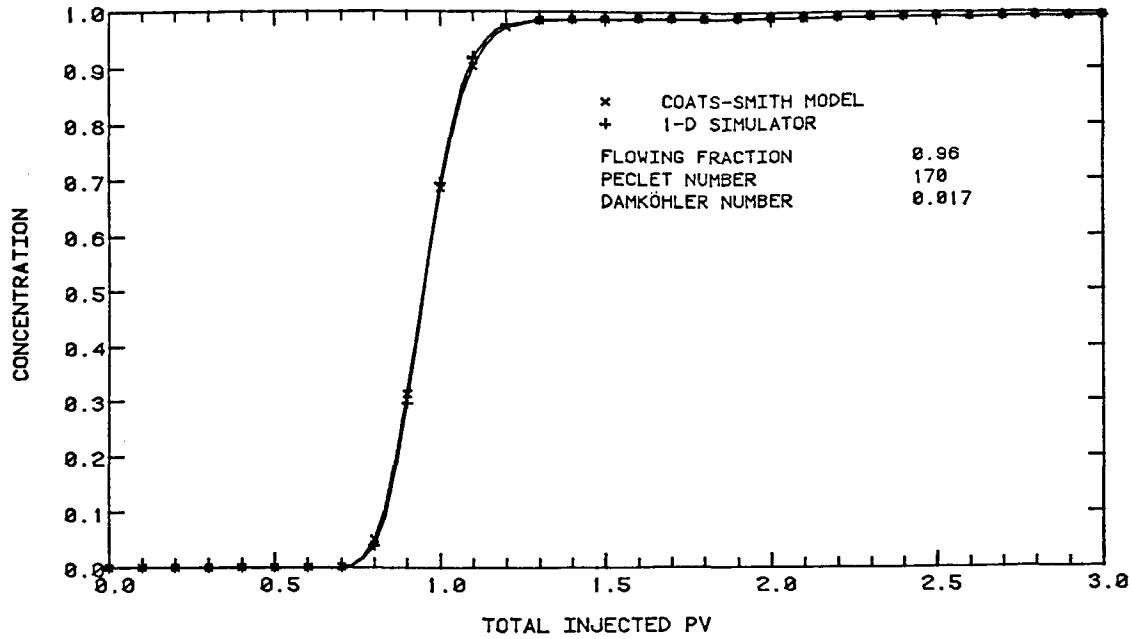

Fig. 5.7 Comparison of the effluent composition solutions for the Coats-Smith model calculated with the one-dimensional simulator with that reported by Coats and Smith (1964).

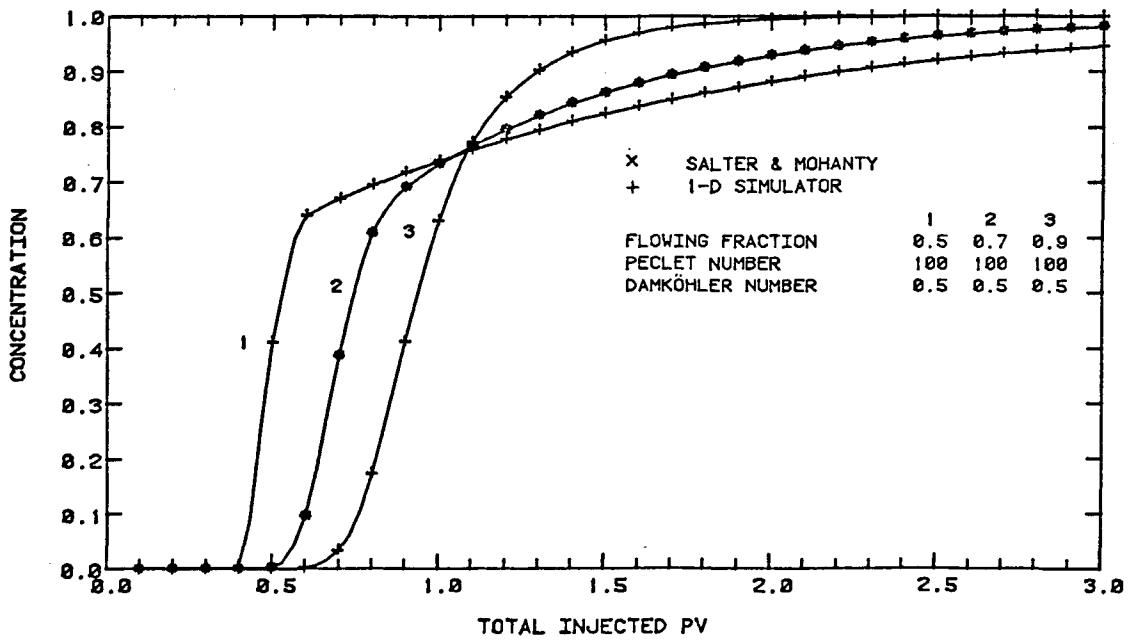

Fig. 5.8 Comparison of effluent composition solutions for the Coats-Smith model calculated with the one-dimensional simulator with those reported by Salter and Mohanty (1982).

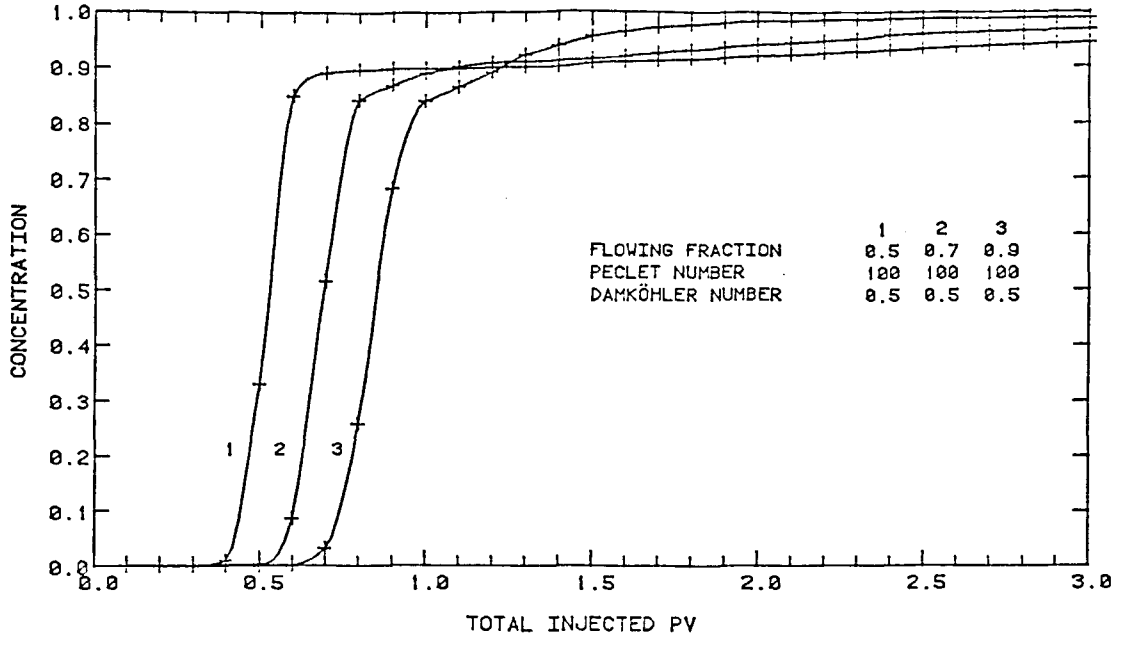

Fig. 5.9 Effect of variations in flowing fraction on calculated effluent compositions in a displacement of Maljamar crude oil by CO_2 at 90°F and 1200 psia.

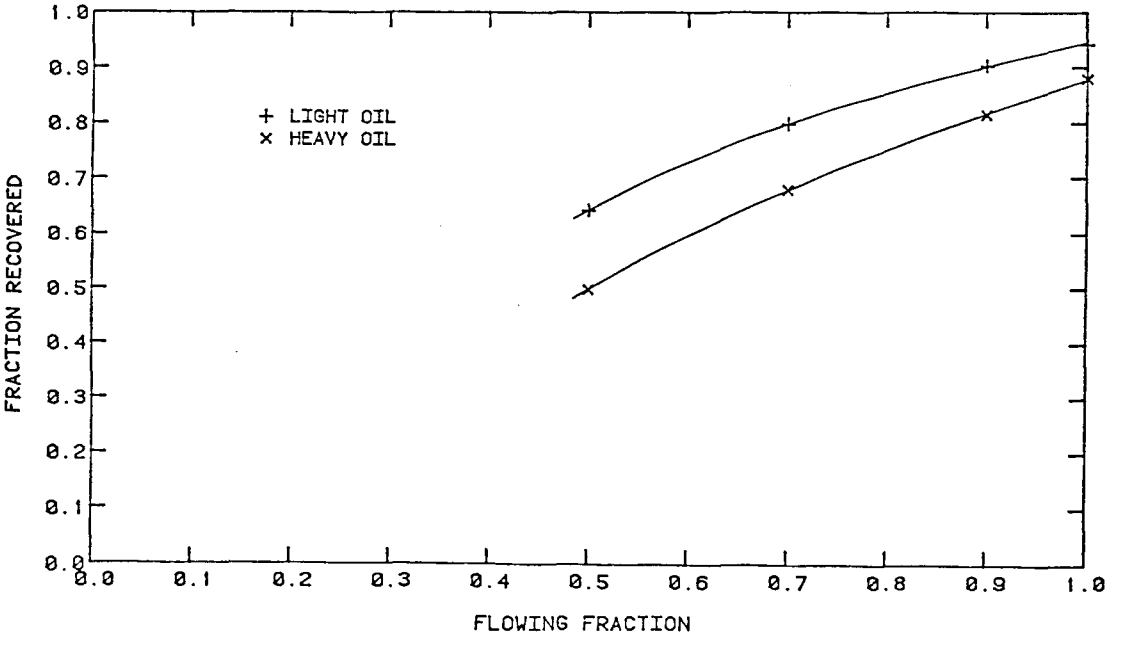

Fig. 5.10 Effect of variations in flowing fraction on calculated oil recovery at 1.2 PV injected.

concentrations in the miscible case. That behavior results from the low viscosity of the CO_2-rich phase. Once the CO_2-rich phase appeared, it flowed more rapidly than did the miscible fluids with unit viscosity ratio.

The effect of changing the flowing fraction on the amount of oil recovered at 1.2 PV injected is shown in Fig. 5.10. In all three displacements, all of the light hydrocarbon component would eventually be recovered by extraction if the displacements were continued long enough. The heavy hydrocarbon component, however, would not. Thus, a decrease in the flowing fraction, with other factors held constant, leads to an increase in the residual saturation to a CO_2 flood. Plots of saturations of CO_2 and oil-rich phases, shown in Fig. 5.11, confirm that the remaining oil saturation is higher when the flowing fraction is low in both the flowing and dendritic fractions. The reason for the differences in saturation in Fig. 5.11 is illustrated in Figs. 5.12 and 5.13, which show composition paths of fluids in the flowing fraction in the middle and outlet grid blocks. When the flowing fraction was 0.7, the composition paths fell relatively close to the dew point portion of the binodal curve. When the flowing fraction was 0.5, the composition paths fell deeper into the two-phase region as heavy components from the dendritic fraction moved by mass transfer into the flowing fraction. That created more oil-rich phase which had very low or zero relative permeability. Thus, the change in the time scale of mixing caused by the presence of a dendritic fraction alters the composition path and hence the efficiency of the displacement in the flowing fraction. In addition, recovery of oil from the dendritic fraction is less efficient than recovery from the flowing fraction.

The effects of changes in the level of dispersion are shown in Fig. 5.14. The effect of increasing dispersion (decreasing Peclet number), with other factors constant, is the same as that described by Gardner, Orr and Patel (1981), and Orr, Yu and Lien (1981). More dispersion causes earlier breakthrough and recovery is lower as is shown in Fig. 5.15. Recovery is much less sensitive to changes in the Peclet number than it is to the flowing fraction, however, as comparison of Figs. 5.15 and 5.10 indicates.

Effects of changes in the rate of mass transfer are shown in Fig. 5.16. High mass transfer delays breakthrough of CO_2 as it transfers more rapidly into the dendritic fraction. Recovery also increases with the mass transfer coefficient, as Fig. 5.17 indicates. As with dispersion, recovery is less sensitive to changes in the rate of mass transfer than to changes in the flowing fraction. That behavior is due to compensating factors which arise from the interaction of phase behavior and mass transfer. When mass transfer is very slow ($a = 0.05$), it is almost as if the dendritic fraction is not present. The displacement in the flowing fraction is efficient because extraction generates miscibility and the remaining oil saturation is low, as is shown in Fig. 5.18a. When the rate of mass transfer is increased (Fig. 5.18b), more oil transfers from the dendritic fraction. Some of that oil is recovered, but the residual oil saturation in the flowing fraction increases as some of the heavy component from the dendritic fraction causes additional oil-rich phase to form. When the mass transfer rate is very high (Fig. 5.18c), mixing between the dendritic and flowing fractions is fast enough, that the multiple contact extraction process operates just as it does when

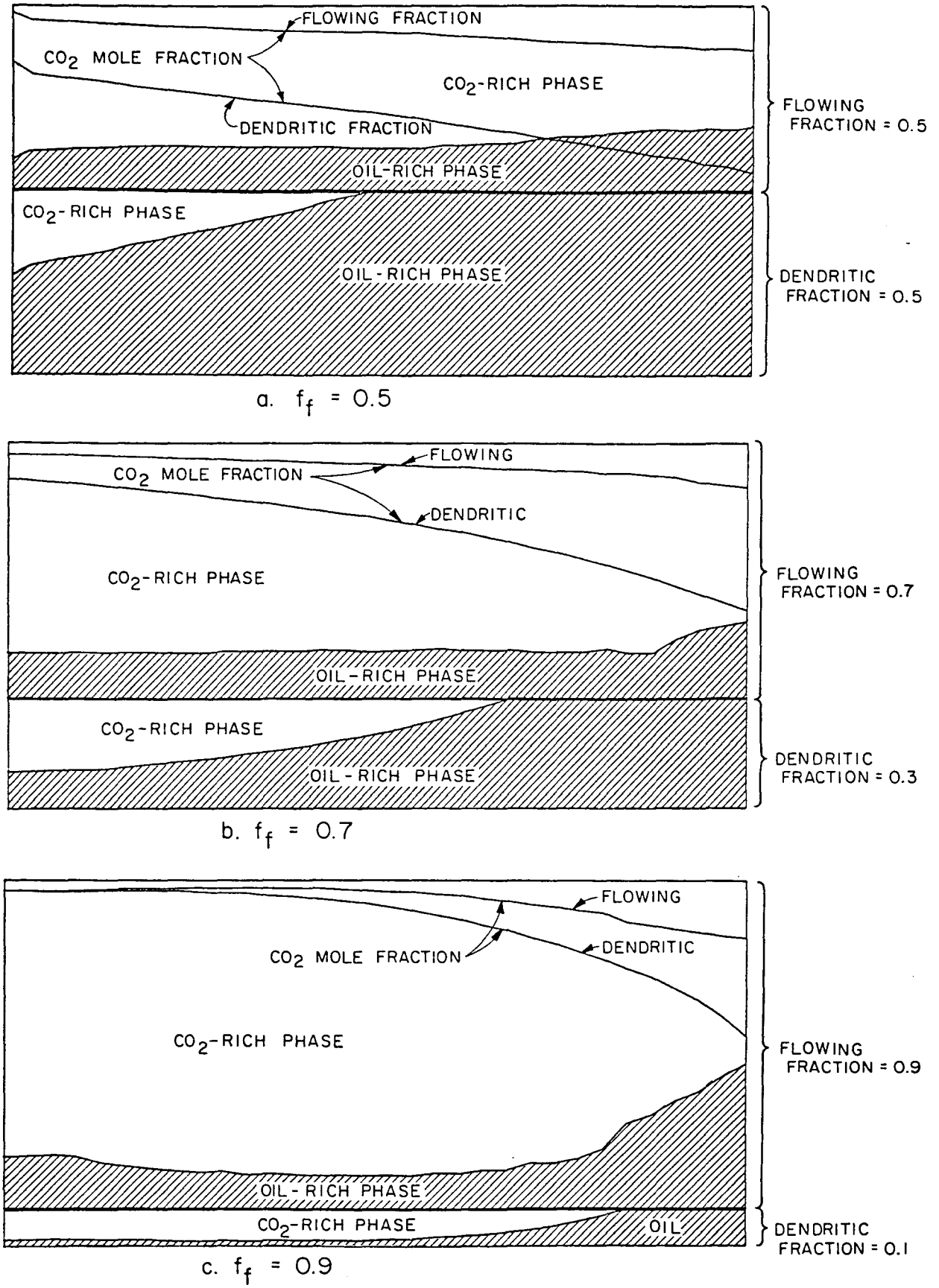

Fig. 5.11 Effect of variations in flowing fraction on remaining oil saturations for displacements of Maljamar crude oil by CO_2 at 90°F and 1200 psia.

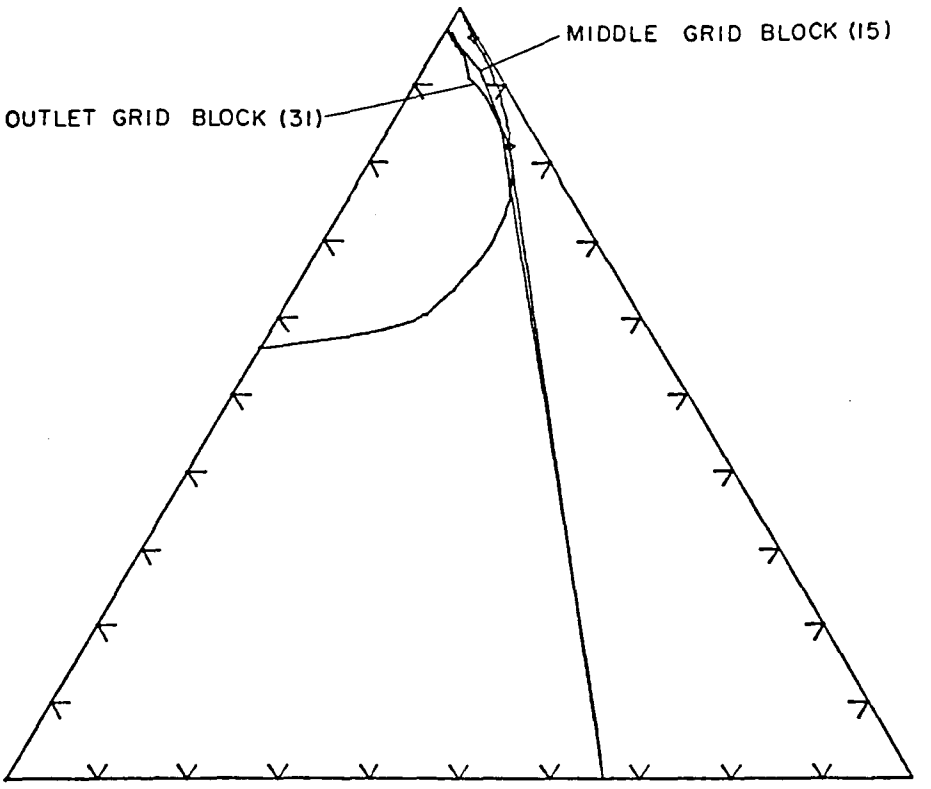

Fig. 5.12 Composition path of fluids in the flowing fraction in the middle and outlet grid blocks for $f_f = 0.7$.

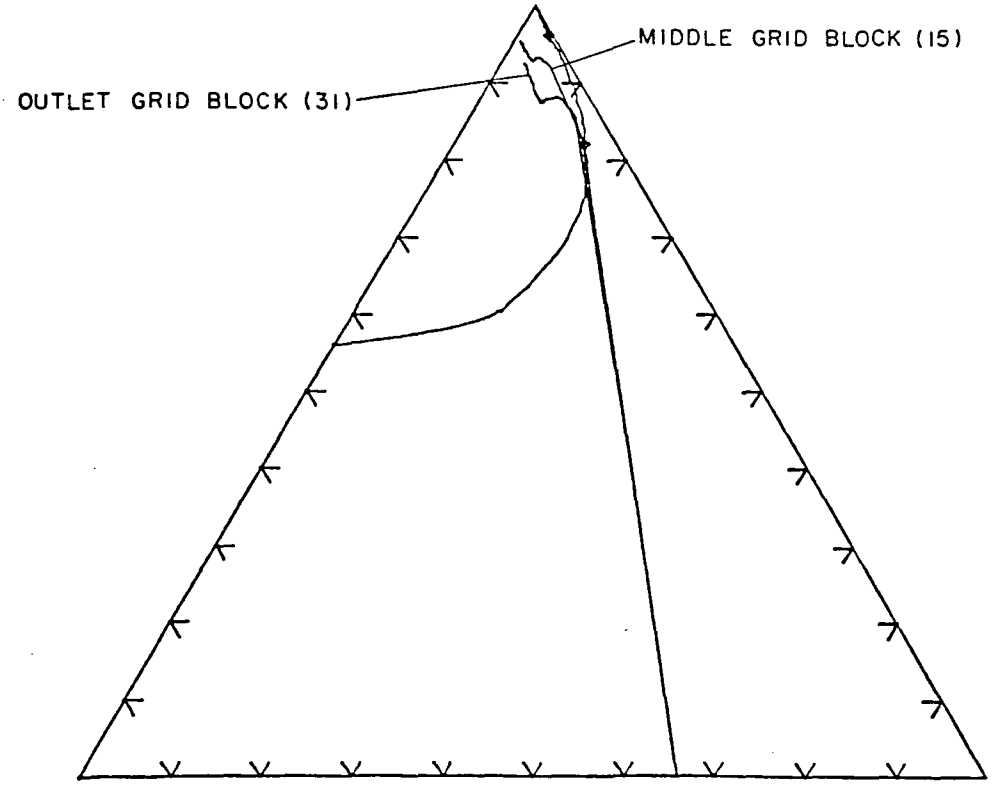

Fig. 5.13 Composition path of fluids in the flowing fraction in the middle and outlet grid blocks for $f_f = 0.5$.

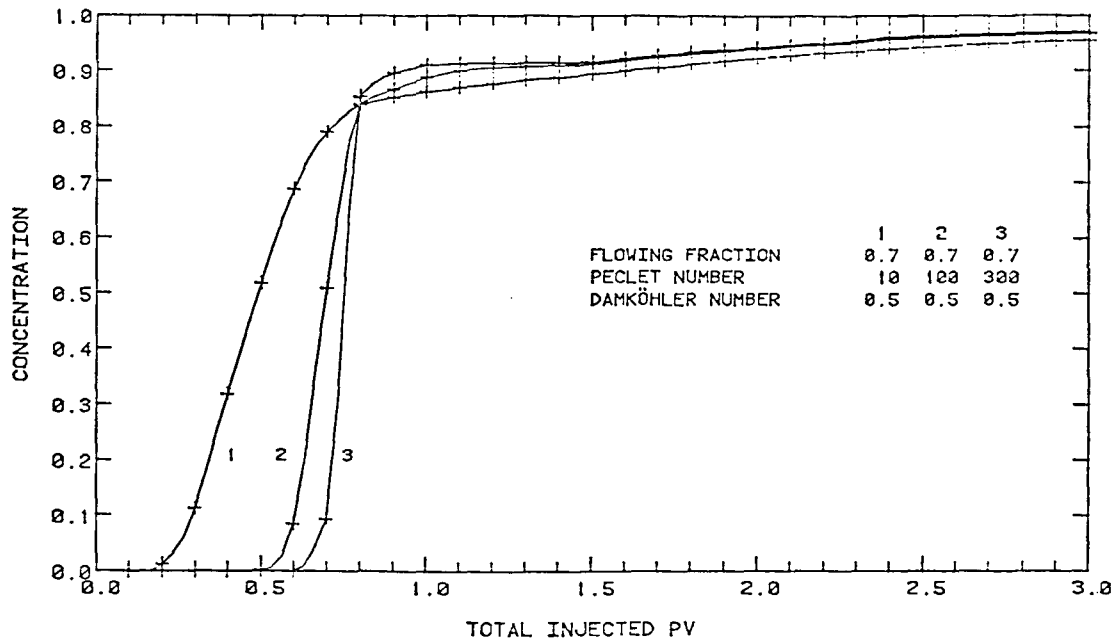

Fig. 5.14 Effect of variations in Peclet number on calculated effluent compositions in displacements of Maljamar crude oil by CO_2 at 90°F and 1200 psia.

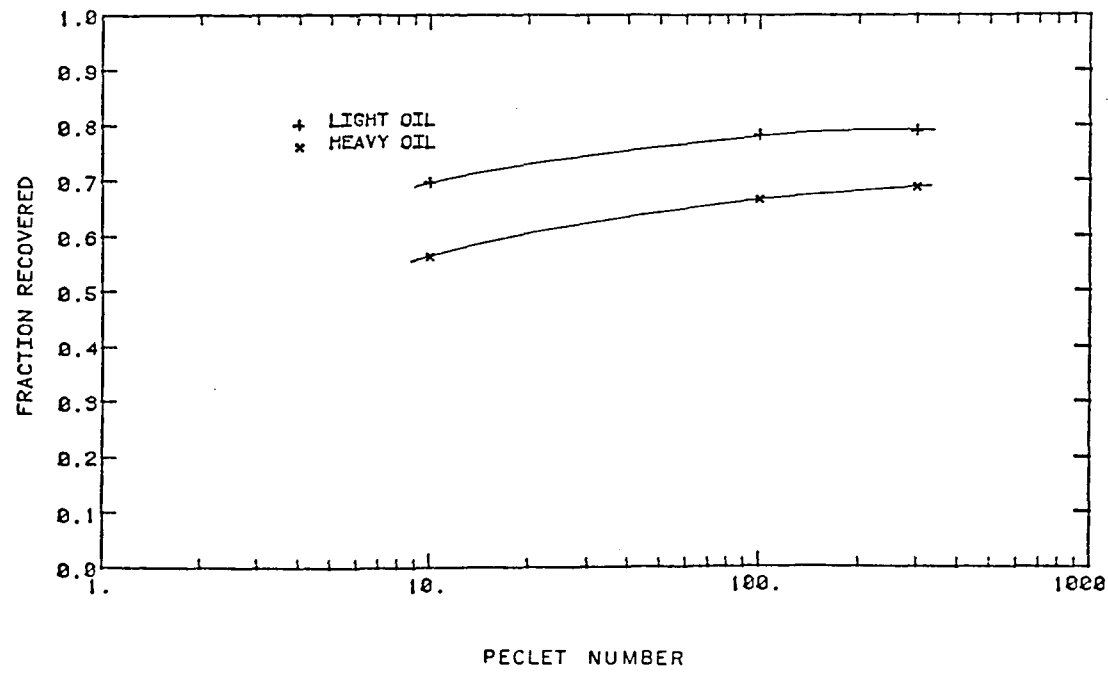

Fig. 5.15 Effect of variations in Peclet number on calculated oil recovery at 1.2 PV injected.

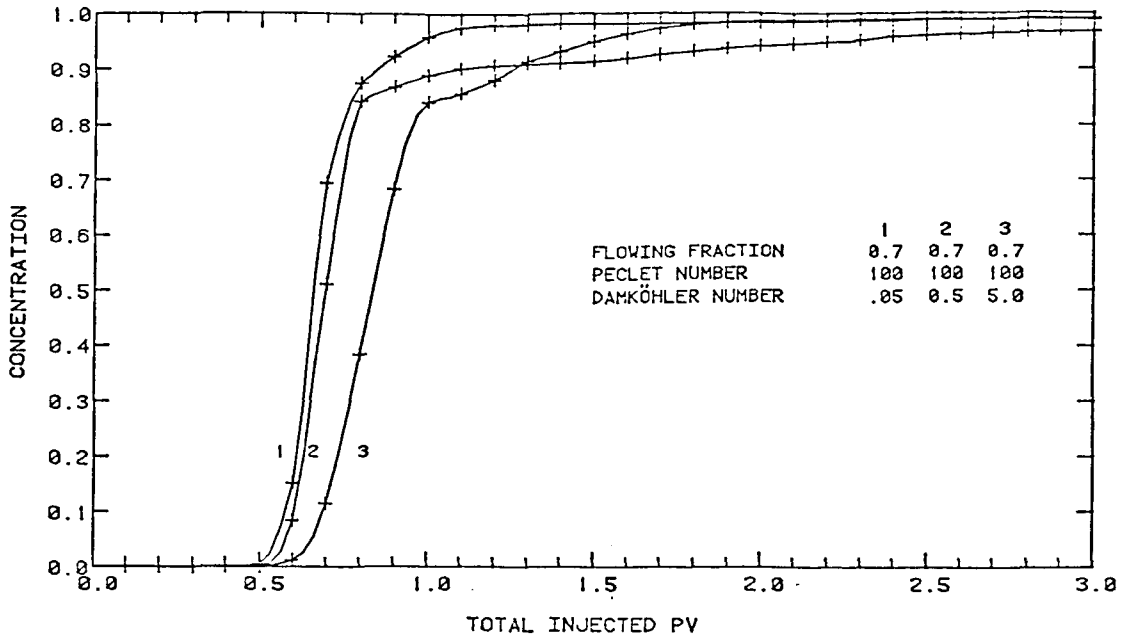

Fig. 5.16 Effect of variations in the rate of mass transfer on calculated effluent compositions in displacements of Maljamar crude oil by CO_2 at 90°F and 1200 psia.

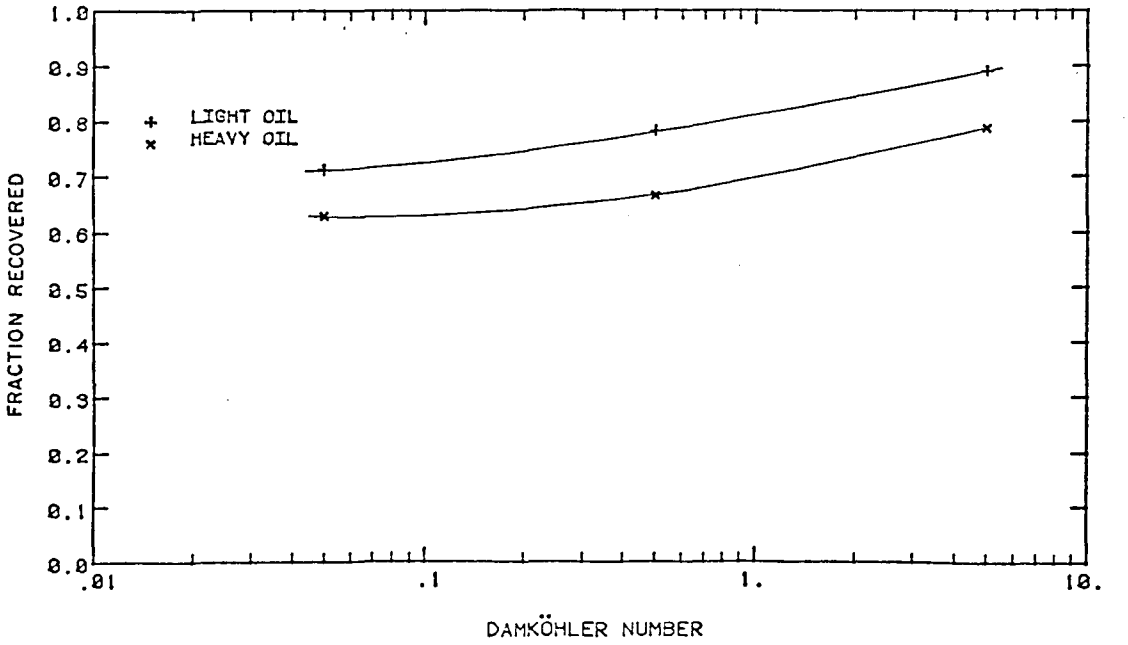

Fig. 5.17 Effect of variations in mass transfer rate on calculated oil recovery at 1.2 PV injected.

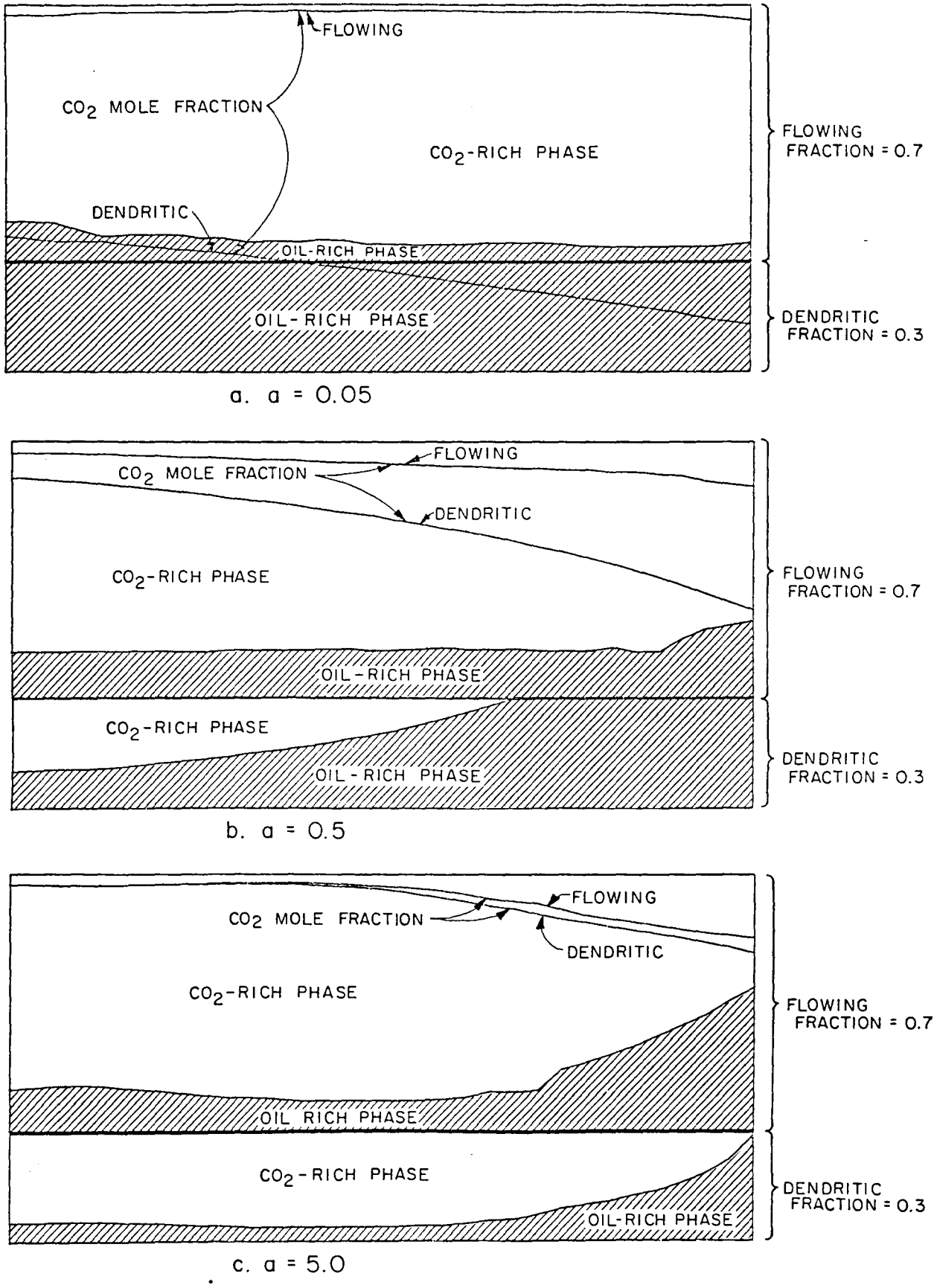

Fig. 5.18 Effect of variations in rate of mass transfer on remaining oil saturations for displacements of Maljamar crude oil by CO_2 at 90°F and 1200 psia.

there is no dendritic fraction present. Clearly, efficient local mixing improves recovery when phase behavior is important.

High Water Saturations

To investigate the impact of high water saturations, simulations of both secondary and tertiary displacements of Maljamar crude oil by CO_2 at 800, 1000 and 1200 psia and 90°F were performed. Gas-oil and water-oil relative permeability reported by Corey (1956), as shown in Fig. 5.19, were used. The original relative permeability curves were rescaled slightly to match the end point saturations reported by Salter and Mohanty (1982). Measured values of the flowing, dendritic and trapped fractions as a function of water saturation in a Berea sandstone core reported by Salter and Mohanty (1982) were used. Those data are given in Fig. 5.20. Mass transfer coefficients measured by Salter and Mohanty were also used (Fig. 5.21). For computational convenience, the number of grid blocks and the time step size were fixed at 50 and 0.000625, which resulted in a Peclet number around 110.

Results of secondary displacements are shown in Figs. 5.22 and 5.23. Fig. 5.22 compares the recovery of light (L) and heavy (H) components obtained in simulations with the original model (§ 5.1), which treats all fluids in a grid block as well mixed, with those obtained with the more complex version which models effects of dendritic and trapped saturations. Results of five displacements at each pressure with each model are shown. In them the fraction of water in the injected fluid varied from zero to one. In the displacements in which CO_2 and water were both injected, alternating slugs of 0.2 PV were used. Recoveries reported in Fig. 5.22 are at one pore volume total injection of CO_2 and water.

At 800 psia, alternate injection of water improved recovery of the immiscible displacement simulated with the well mixed version of the model because the mobility of the CO_2 was reduced. When pure CO_2 was injected, the immiscible displacement was relatively inefficient because the CO_2 mobility was high. Just as in a Buckley-Leverett calculation for low viscosity water displacing high viscosity oil, little additional oil was recovered after CO_2 breakthrough. Despite the solubility of CO_2 in the oil, a straight waterflood was more effective than continuous CO_2 injection. Because the only compositional effect present was the solubility of the CO_2 in the oil, there was no difference in recovery between the light and heavy components. When both CO_2 and water were injected, swelling of oil by dissolved CO_2 along with the CO_2 mobility reduction caused higher recovery. A straight waterflood was as effective, however. When effects of trapped and dendritic saturations were included, however, the benefits of the mobile water saturation were reduced as the water interfered with mixing of CO_2 and the oil. In this immiscible displacement, alternate injection of CO_2 and water was no better than a waterflood when effects of trapped and dendritic saturations were included.

At the higher injection pressures (1000 and 1200 psia), phase behavior had a larger effect. In all the cases, injection of CO_2 with the water recovered more oil than a waterflood, as did continuous CO_2 injection. Recoveries of light and heavy components differed due to preferential

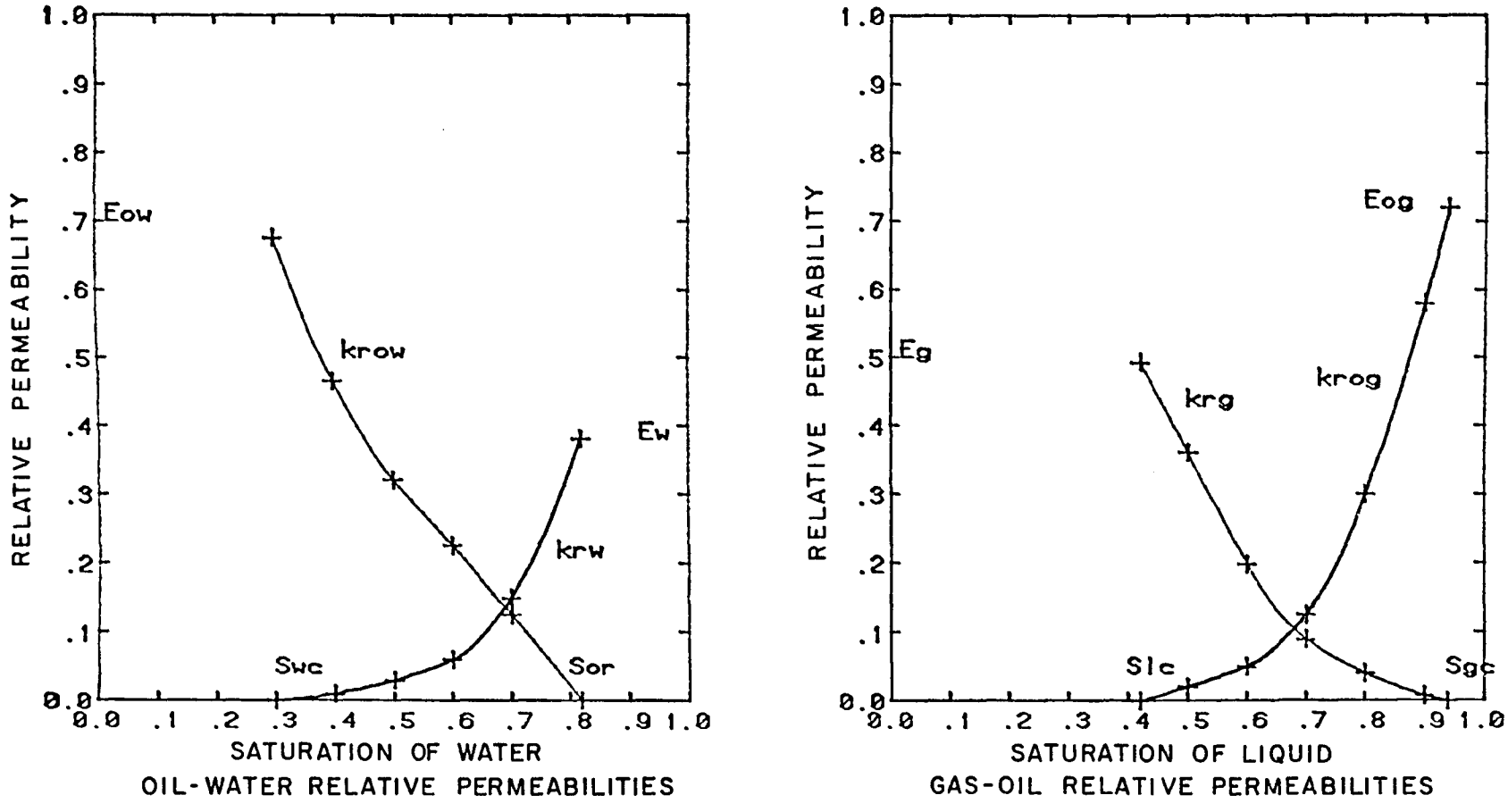

Fig. 5.19 Relative permeability functions for simulations of the effect of high water saturations.

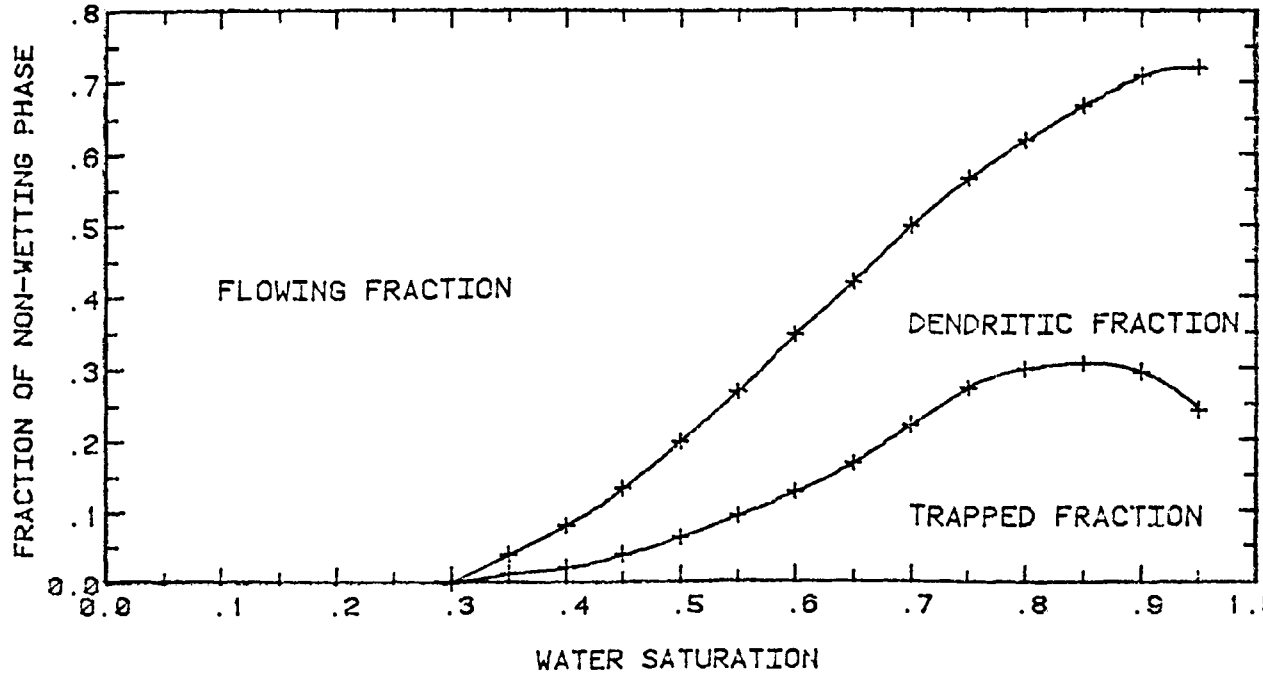

Fig. 5.20 Dendritic and trapped fractions reported by Salter and Mohanty (1982).

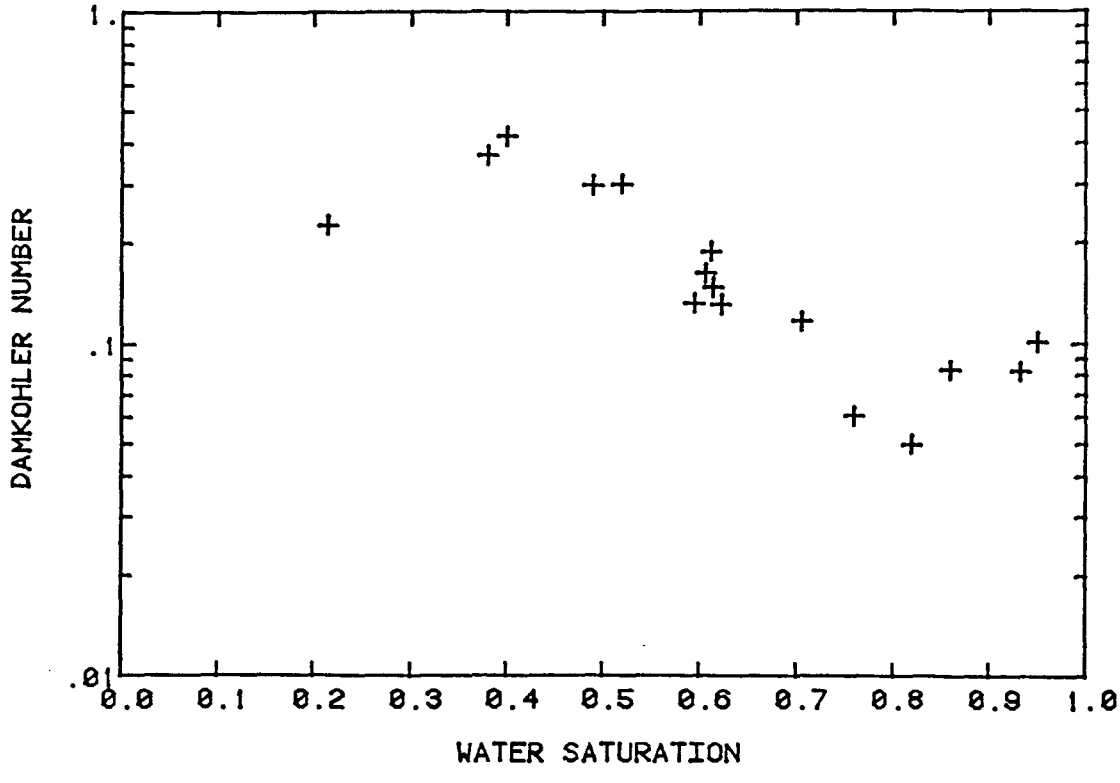

Fig. 5.21 Rate of mass transfer as a function of water saturation (Salter & Mohanty 1982).

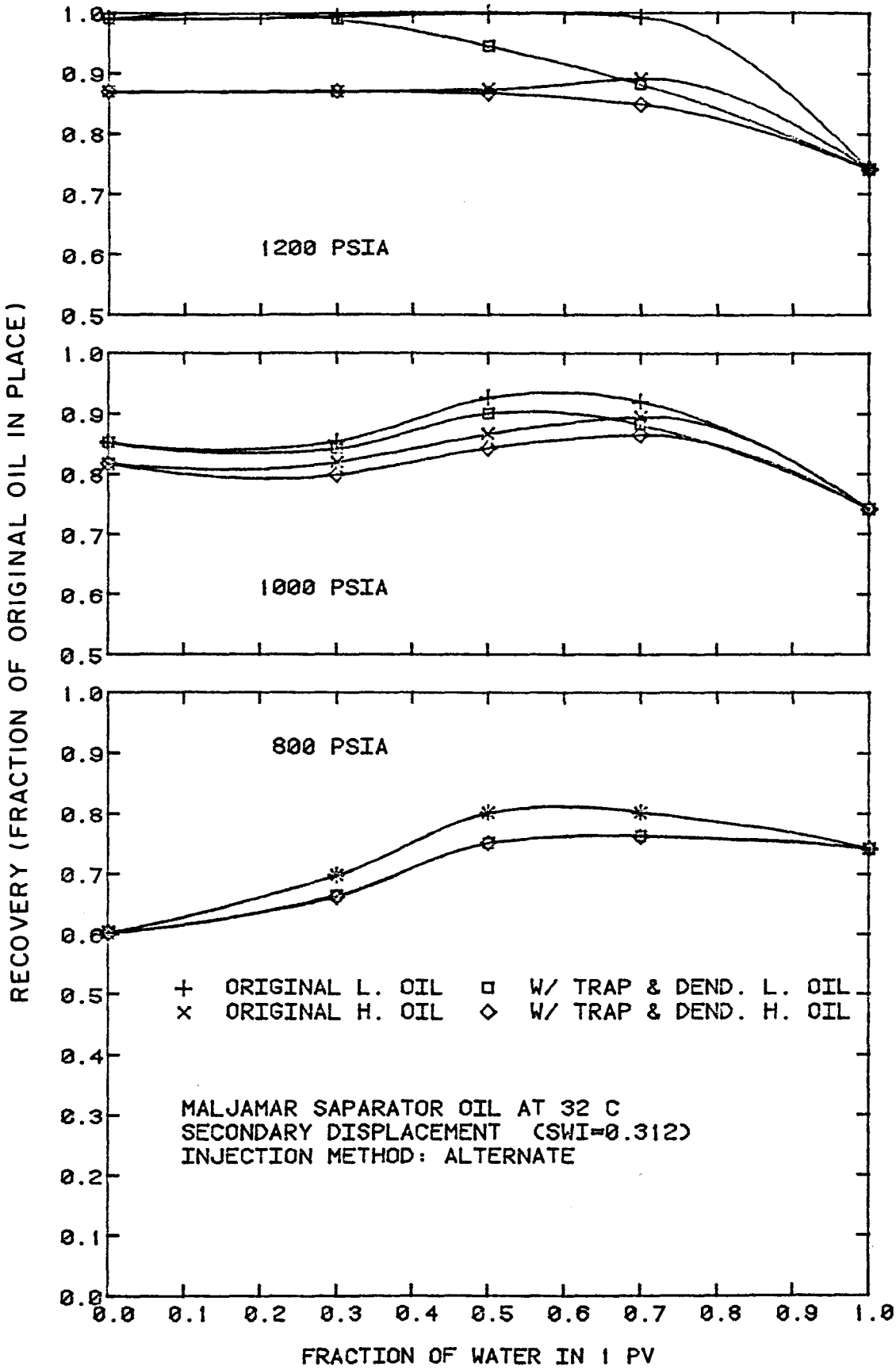

Fig. 5.22 Calculated oil recovery at one pore volume total injection in secondary displacements of Maljamar crude oil by CO_2. CO_2 and water were injected in alternate slugs of 0.2 PV.

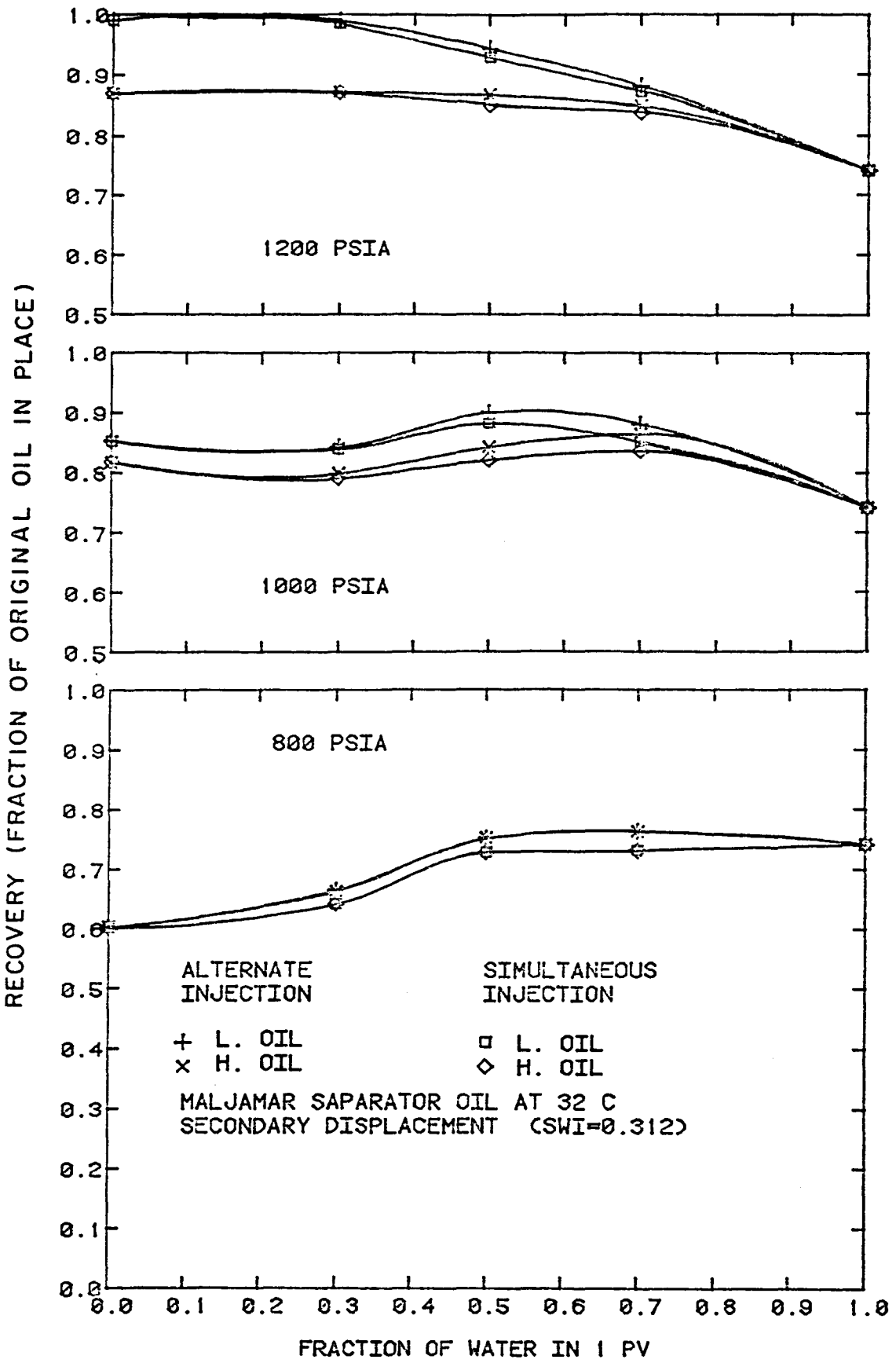

Fig. 5.23 Comparison of alternate and simultaneous injection in secondary displacements.

extraction of the light hydrocarbons. At 1000 psia, alternate water injection provided some benefits if fluids were completely mixed, but the improvement in recovery was reduced when effects of trapped and dendritic fractions were included. At that pressure, however, the difference in recovery between the two cases was relatively small. Recovery increased slightly with the volume fraction of water in the injection stream, as long as some CO_2 was injected. At 1200 psia, nearly all of the light component had been recovered at 1.0 PV injected when CO_2 was injected continuously. When the fluids were treated as well mixed, recovery of both heavy and light components stayed high as the volume fraction of water increased. When dendritic and trapped fractions were included, however, recovery of both components was lower, as less favorable mixing behavior altered the fraction of oil contacted and the local composition path. Thus, oil recovery was most sensitive to the amount of water in the injection stream when phase behavior (extraction) had the largest impact on displacement efficiency.

The performance of secondary displacements in which CO_2 and water were injected simultaneously is compared with that of alternate slug injection in Fig. 5.23. The oil recovery results shown were calculated with the effects of trapped and dendritic saturations included. If, instead, fluids are assumed to be well mixed, there is no difference between the two injection methods as long as there is no relative permeability hysteresis. At all three pressures, there was very little difference between the two injection methods. Where differences were observed, alternate injection performed slightly better. When water and CO_2 were injected simultaneously, water saturations stayed approximately constant in the swept zone. When alternate injection was used, the resulting variations in water saturation allowed CO_2 to contact slightly more oil.

Effects of restrictions to mixing in tertiary floods with alternate injection of CO_2 and water are shown in Fig. 5.24. At 800 psia, some oil was recovered when fluids were assumed to be well mixed because the CO_2 dissolved in the oil and swelled it enough that it had nonzero relative permeability. When trapping was included, however, no additional oil was recovered. Evidently, the swelling of the limited amount of oil contacted was not sufficient to produce significant oil recovery at one pore volume injected. At the higher pressures, where extraction was more efficient, recovery was also higher. When the fluids were assumed to be well mixed, there was almost no effect of the ratio of water to CO_2 in the injection stream, and recovery was high. When dendritic and trapped saturations were included, much less oil was recovered. At both 1000 and 1200 psia, recovery declined as the fraction of water in the injected fluid increased. As the water fraction increased, so did the water saturation, which decreased the amount of oil contacted by the CO_2. Thus, performance of tertiary floods was much more sensitive to the presence of water than were secondary floods, and performance was reduced most by the water when phase behavior contributed most to recovery in the well-mixed case.

Fig. 5.25 compares performance of simultaneous and alternate injection methods. At 800 and 1000 psia there was essentially no difference between the methods. At 1200 psia, alternate injection was slightly more effective, but in both cases continuous CO_2 injection performed better. It should be noted,

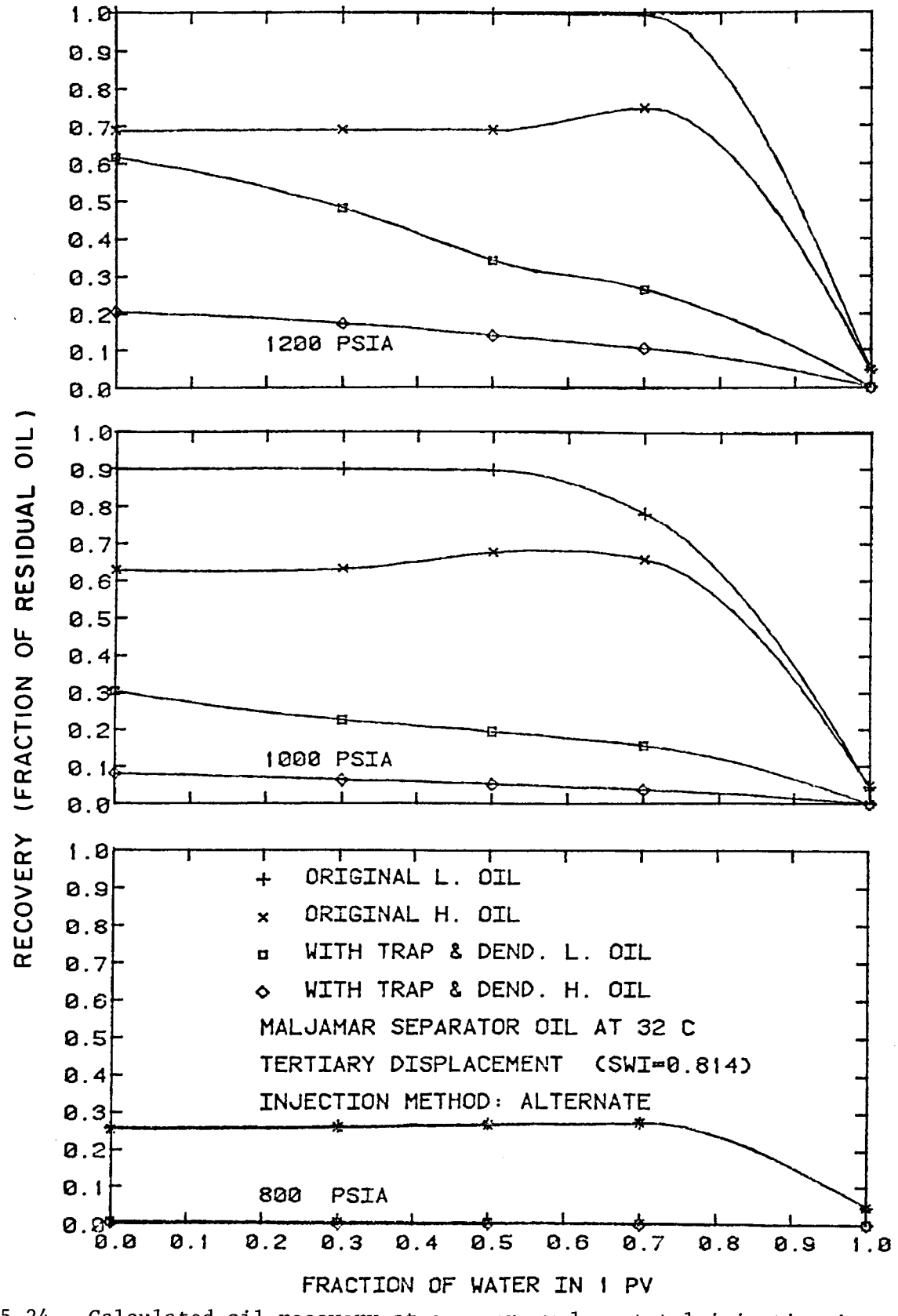

Fig. 5.24 Calculated oil recovery at one pore volume total injection in tertiary displacements of Maljamar crude oil by CO_2. CO_2 and water were injected in alternate slugs of 0.2 PV.

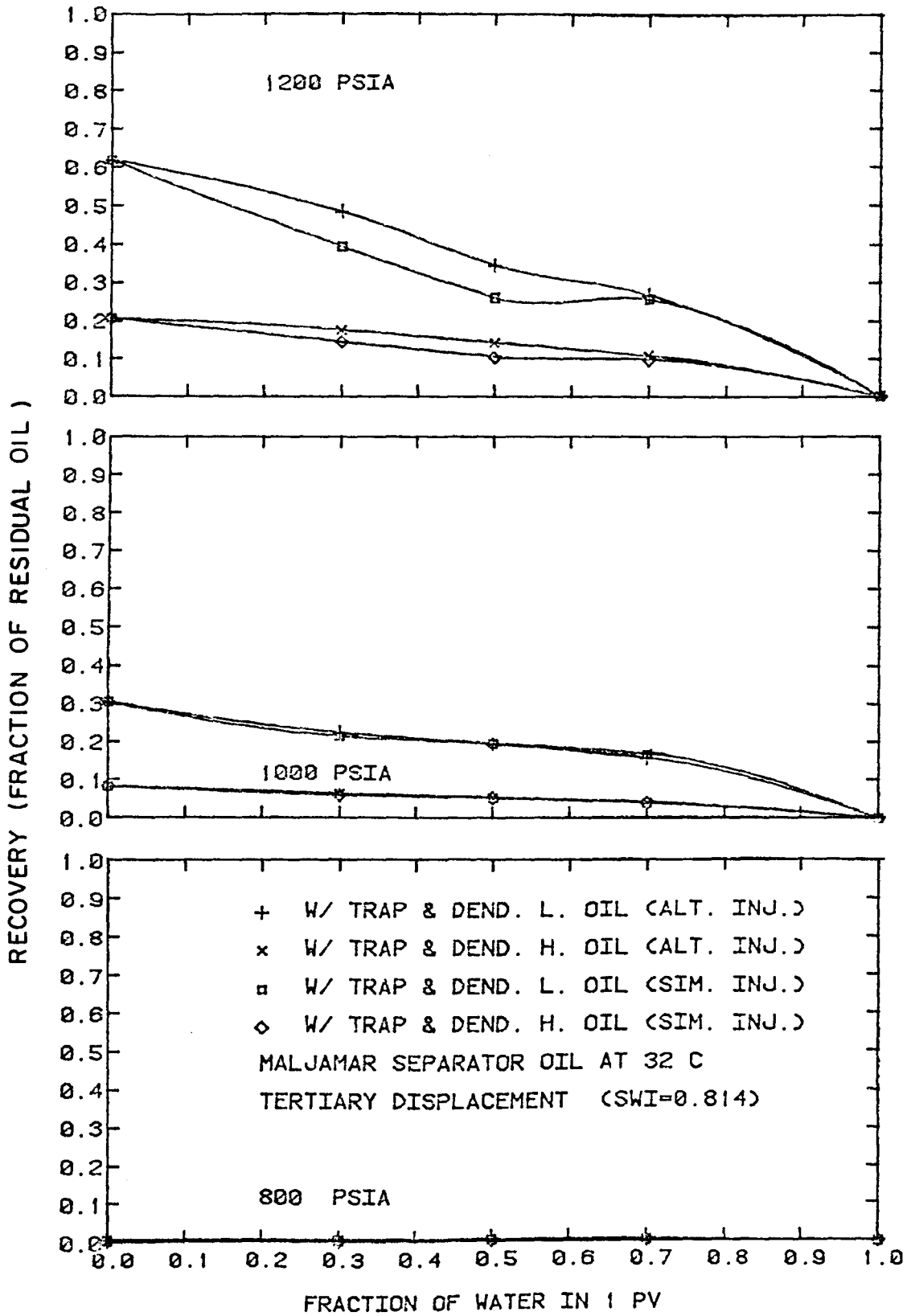

Fig. 5.25 Comparison of alternate and simultaneous injection in tertiary displacements.

however, that the principal reason for injecting water would be to reduce the impact of viscous instability. Since viscous instability was not modeled in the one-dimensional displacements reported here, these simulations do not allow an assessment of the trade-off between the benefits of mobility control and the adverse effects of restrictions to mixing. These results do illustrate the potential impact of the restrictions to mixing which can occur due to high water saturations in a water-wet porous medium. Such restrictions will inevitably act to reduce recovery to some extent in a CO_2 flood. In oil-wet rocks, both core floods (Tiffin & Yellig 1983) and the flow visualizations of §3 suggest that mixing of oil and CO_2 will be more efficient than in strongly water-wet rocks, though little is known about mixing in multiphase flow in the heterogeneous pore structures found in some carbonates. Thus, the results presented here represent only a first step toward quantitative assessment of the interactions of mixing, flow and phase behavior in reservoir rocks.

5.4 Conclusions

The simulation results presented here indicate that:

(1) Displacement of oil by CO_2 in a slim tube is efficient when extraction of hydrocarbons by a CO_2-rich phase is efficient.

(2) Efficient extraction accounts for the high oil recovery observed in slim tube displacements. Increases in the density and viscosity of CO_2 with increasing pressure in the absence of extraction do not.

(3) Quantitative predictions of slim tube performance can be obtained based on simple representations of phase composition and density data obtained from the continuous multiple contact experiment.

(4) Significant microscopic pore structure heterogeneity, of the type characterized by a flowing fraction less than one in the Coats-Smith model, leads to reduced recovery in multicontact miscible CO_2 floods without water present because less efficient mixing between fluid in preferential flow paths and fluid in other parts of the pore space alters local composition paths in an adverse way.

(5) Calculated oil recovery in CO_2 floods without water present is less sensitive to variations in the Peclet and Damköhler numbers observed in typical laboratory core displacements than to variations in the flowing fraction.

(6) Comparison of simulations of secondary and tertiary laboratory core floods in which fluids were assumed to be locally well mixed with those in which the effects of trapped and dendritic saturations were represented indicate that restrictions to mixing caused by high water saturations in water-wet porous media, slow mass transfer to and from dendritic pore space and an isolated or trapped fraction,

also act to reduce oil recovery. Calculated recovery was most sensitive to the presence of water when extraction was most efficient. In one-dimensional flows, those adverse effects partly negate the benefits of mobility control from the high water saturations. Additional work is needed to assess quantitatively the trade-off between the improved sweep obtained with the mobility control induced by high water saturations and the resulting lower local displacement efficiency in multidimensional flows.

6. SUMMARY

This report summarizes progress in a comprehensive research effort to build understanding of the factors which influence CO_2 flood performance. Results are reported in four areas:

(1) Measurement and prediction of phase behavior and fluid properties for CO_2-hydrocarbon systems.

(2) Flow visualizations for immiscible, first contact miscible and multiple contact miscible displacements.

(3) Measurements of effects of microscopic heterogeneity on mixing during single-phase flow in reservoir cores.

(4) One-dimensional simulation of the interactions of phase behavior, flow and restrictions to local mixing due to dendritic and trapped fractions in the nonwetting phase.

In the first area, results of a variety of measurements of CO_2-hydrocarbon phase behavior are reported. Pressure composition phase diagrams for nine oils are presented which indicate clearly the effects of changing system temperature and adding solution gas to an oil. Because different oil fields have been subjected to widely varying pressure histories and because amounts of gas present initially vary widely, gas-oil ratios for fields to be CO_2 flooded will also vary widely. The results given here outline effects of a change in the gas-oil ratio for oils similar in composition. Also given is a simple physical explanation for the temperature dependence of empirical minimum miscibility correlations. Results of experiments with nitrogen contaminated CO_2 outline clearly the adverse effects of the addition of components to the CO_2 which lower its density. A simple procedure for estimating the effects of changes in system temperature or of the addition of contaminants to the CO_2 was given. It too is based on the idea that efficient extraction of hydrocarbons from the oil requires some characteristic CO_2 density.

Measurements of component partitioning between CO_2 and oil-rich phases for paraffinic, aromatic and naphthenic hydrocarbons indicate that for oils with approximately the same molecular weight distribution, branched alkanes are extracted most effectively followed by normal alkanes, aromatics and naphthenes. The results of those experiments point the way to additional experiments needed to delineate the effects of crude oil composition on minimum miscibility pressure.

Comparison of phase compositions calculated with the Peng-Robinson equation of state with measured values indicates that the equation is both qualitatively and quantitatively accurate for systems showing the complex liquid-vapor, liquid-liquid and liquid-liquid-vapor of many CO_2-hydrocarbon systems at low temperatures. The agreement between calculated and measured phase behavior for well-characterized hydrocarbon systems, at least, is good

enough that evolution of phase diagrams in temperature or pressure can be studied more efficiently with the equation of state than with expensive and time-consuming experiments.

Finally, it was shown that the viscosities of high pressure fluids can be measured accurately with a viscometer based on an oscillating quartz crystal. With such a device mounted in the sample production lines of the continuous multiple contact apparatus, simultaneous measurement of compositions, densities and viscosities of two phases in equilibrium should be possible.

In the second area, flow visualization experiments for immiscible, first contact miscible and multiple contact miscible secondary and tertiary CO_2 floods were described. The displacements were performed in two-dimensional pore networks etched in glass. While the displacements were not scaled to represent flow in reservoir rocks, they did indicate that dense CO_2 could recover nearly all the oil it contacted. Low density CO_2 displaced oil nearly as inefficiently as low density nitrogen even though it was about six times more soluble in the oil than nitrogen. When the water saturation was high, dense CO_2 did not displace oil effectively when the pore network was water-wet. When it was oil-wet, however, dense CO_2 contacted and displaced most of the oil because continuous, oil-filled flow paths existed in the capillary grooves at the edges of the pores. Finally, observation of interfaces surrounding trapped oil blobs clearly showed that CO_2 can diffuse through water to reach trapped oil. Those observations suggested a simple experiment for the measurement of diffusion coefficients in CO_2-oil-water systems.

In area (3), experiments to examine the effects of microscopic (pore level) restrictions to the mixing of CO_2 and oil were performed. It was shown that mixing in single-phase displacements in three sandstones and one carbonate core sample was relatively efficient. In those displacements, the growth of the transition zone between injected and displaced fluid could be modeled by dispersion alone. In three other carbonate samples, however, local mixing was less efficient. Injected fluid appeared at the outlet at significantly less than one pore volume injected and significant tailing was observed. Examination of thin sections indicated that such mixing effects were the result of the much wider distribution of pore sizes present in those carbonates coupled with the fact that the pores were connected in ways that generated preferential flow paths. The slow exchange of fluid between that in the preferential flow paths and that in the smaller pores generated effluent fluid compositions which could be modeled by the three parameters of the Coats-Smith model, a flowing fraction, a dispersion coefficient and a mass transfer coefficient.

The interactions of such restrictions to mixing at the microscopic level with the phase behavior of CO_2-crude oil mixtures was examined in the last area. A one-dimensional simulator which models the effects of phase behavior and volume change on mixing and assumes that fluids are locally well mixed was used to simulate slim tube displacement experiments based on independent measurements of phase behavior and fluid properties obtained in continuous multiple contact experiments. Prediction and experiment agreed well enough to suggest that the theory of stable, one-dimensional displacements is well

understood, despite the complexity of CO_2-crude oil phase behavior. Modifications to the simulator to model the effects of microscopic restrictions to mixing, the result of heterogeneity of the pore structure or high water saturations, were described. Simulations of CO_2-crude oil displacements indicated that one effect of restricted mixing is to alter local composition paths in a way that reduces local displacement efficiency.

Thus, this report summarizes progress in a systematic effort to understand and quantify factors which determine CO_2 flood performance. As with any account of a continuing research program, it raises as many questions as it answers. It represents, therefore, the basis for additional work toward the goal of more accurate prediction of CO_2 flood performance at field scale.

ACKNOWLEDGEMENT

The support that made this research effort possible was provided by the U.S. Department of Energy, the New Mexico Energy Research and Development Institute and a consortium of companies and foundations including the Abu Dhabi Reservoir Research Foundation, American Cyanamid, the Amoco Foundation, ARCO Oil and Gas, Conoco, Marathon, Mobil, Shell Development, Sohio, Sun Exploration and Production, and Tenneco. That support is gratefully acknowledged. In addition, support was provided by the Petroleum Recovery Research Center.

Core and crude oil samples used in this study were provided by Amerada Hess, ARCO, Conoco, and Shell. Equipment grants from Amoco, ARCO, Conoco, Chevron, and Sun were used for analytical, microcomputer and data acquisition equipment. That support made possible the high quality instrumentation which contributed materially to this project. Without it, progress would have been much slower.

This report is based on much hard work by students and staff at the Petroleum Recovery Research Center. Mark Taylor and Claire Jensen did the static equilibrium phase behavior experiments with CO_2 and N_2. Matthew Silva supervised the development and operation of the continuous multiple contact experiment. Chris Lien supervised the analytical work so important to that experiment. Mickey Pelletier and Joe Franklin designed the data communications system and Joe Franklin wrote most of the code for the computer control system. Frank Shelley and Cynthia Hutter also assisted with the programming chores. Francisco Romero and Pat Rosacker also assisted with the CMC experiments. Leopoldo Larsen did the equation of state calculations. Mickey Pelletier designed, built and tested the quartz crystal viscometer. The flow visualization apparatus was built by Bruce Campbell who also did many of the experiments reported. Ibrahim Bahralolom performed the displacements comparing N_2 and CO_2. Greg Ruskauff is working on the measurement of diffusion coefficients for CO_2 systems. Bob Bretz supervised the core flood experiments with assistance from Mary Graham, Mike Mayer and Steve Welch. The continuous oil-water separator was Bob Bretz's idea. Mickey Pelletier and Steve Welch have built numerous versions of it. Bob Specter did the thin section work. Kar-Keung Dai modified the one-dimensional simulator to include effects of trapped and dendritic oil and ran many simulations. Sections of the text were written by Ibrahim Bahralolom, Bob Bretz, Leopoldo Larsen, Mickey Pelletier, Greg Ruskauff, Matthew Silva, Bob Specter, Mark Taylor and Steve Welch.

Kathy Grattan, Paula Bradley and Jessica McKinnis deserve special thanks for their careful attention to the details of the editing, assembly, and production of this report. Preparation of a report of this size without their skilled assistance would have been difficult indeed.

Our colleagues at the Petroleum Center contributed to this project in many ways. John Heller, Norman Morrow and Dave Martin, and members of their research groups, helped us wrestle with the difficulties that are a normal

part of experimental work and participated in endless discussion of the results and their interpretation. John Chatzis, now with the University of Waterloo, helped us adapt his micromodels to our high pressure application. Jill Ward helped us check wetting behavior in the micromodels and Geoff Mason of Loughborough University helped set us on the right track toward understanding the behavior of fluids in the capillary grooves. Kay Brower of the Chemistry Department at New Mexico Tech suggested the use of sucrose as a tracer. Roger Card of American Cyanamid helped us look at partitioning in CO_2-hydrocarbon systems. Bill Shreve of Hewlett-Packard had crystals made for us and helped us get started in the oscillating quartz crystal work. Finally, Royal Watts, Al Yost, and Fred Burtch of the U.S. Department of Energy, and Leo Noll now with the National Institute for Petroleum Research, who was our technical project officer during most of the project period, deserve thanks for their continued interest in our work.

REFERENCES

Aris, R. and Amundson, N. R. 1957, "Some Remarks on Longitudinal Mixing or Diffusion in Fixed Beds," AIChE J. 3, 280.

Aronofsky, J. S. and Heller, J. P. 1957, "A Diffusion Model to Explain Mixing of Flowing Miscible Fluids in Porous Media," Trans., AIME 210, 345-349.

Baker, L. E. 1977, "Effects of Dispersion and Dead-End Pore Volume in Miscible Flooding," Soc. Pet. Eng J. 17, 219-227.

Baker, L. E., Pierce, A. C., and Luks, K. D. 1982, "Gibbs Energy Analysis of Phase Equilibria," Soc. Pet. Eng. J. 22, 731-742.

Batycky, J. P., Maini, B. B., and Fisher, D. B. 1982, "Simulation of Miscible Displacement in Full Diameter Carbonate Cores," Soc. Pet. Eng. J. 22, 647-658.

Brenner, H. 1962, "The Diffusion Model of Longitudinal Mixing in Beds of Finite Length. Numerical Values," Chem. Eng. Sci. 17, 229-243.

Bretz, R. E., Pelletier, M. T., and Orr, F. M., Jr. 1984, "A Small Volume, Continuous, Oil-Water Separator for Laboratory Displacement Experiments," accepted J. Pet. Tech. (March).

Brigham, W. E., Reed, P. W., and Dew, J. N. 1961, "Experiments on Mixing During Miscible Displacement in Porous Media," Soc. Pet. Eng. J. 1, 1-8.

Campbell, B. T. 1983a, "Flow Visualization of CO_2-Crude Oil Mixtures," M.Sc. Thesis, New Mexico Institute of Mining and Technology, Socorro (May).

Campbell, B. T. 1983b, "Photofabrication of Porous Networks in Two-Dimensional Glass Plate Micromodels," PRRC Report 83-3, Petroleum Recovery Research Center (January).

Campbell, B. T. and Orr, F. M., Jr. 1983, "Flow Visualization for CO_2-Crude Oil Displacements," SPE 11958, presented at 58th Fall Conference of SPE of AIME, San Francisco, October 5-8.

Chatzis, I. 1982, "Photofabrication Technique of 2-D Glass Micromodels of Residual Oil Saturation," PRRC Report 82-12, Petroleum Recovery Research Center (March).

Chatzis, I., Morrow, N. R., and Lim. H. T. 1983, "Magnitude and Detailed Structure of Residual Oil," Soc. Pet. Eng. J. 23, 311-336.

The Chemical Rubber Company 1968, Handbook of Chemistry and Physics, 48th Edition, Cleveland, Ohio.

Coats, K. H. 1979, "An Equation-of-State Compositional Model," SPE 8284, presented at SPE 54th Annual Fall Meeting, Las Vegas, September 23-26.

Coats, K. H. and Smith B. D. 1964, "Dead-End Pore Volume and Dispersion in Porous Media," Soc. Pet. Eng. J. 4, 73-84.

Collings, A. F. and McLaughlin, E. 1971, "Torsional Crystal Technique for the Measurement of Viscosities of Liquids at High Pressure," Trans. Faraday Soc. 67, 340-352.

Concus, P. and Finn, R. 1969, "On the Behavior of a Capillary Surface in a Wedge," Proc., Nat. Acad. Sci. 63, 292-299.

Corey, A. T., Rathjens, C. H., Henderson, J. H., and Wyllie, M. R. J. 1956, "Three-Phase Relative Permeability," Trans., AIME 207, 349-353.

Dai, K. K. 1984, "Numerical Simulation of CO_2-Crude Oil Displacements: Effects of High Water Saturations," M.Sc. Thesis, New Mexico Institute of Mining and Technology, Socorro (May).

Danckwerts, P. V. 1950, "Unsteady-State Diffusion or Heat-Conduction with Moving Boundary," Trans., Faraday Soc. 46, 701-712.

Deans, H. A. 1963, "A Mathematical Model for Dispersion in the Direction of Flow in Porous Media," Soc. Pet. Eng. J. 3, 49.

De Bock, A., Grevendonk, W., and Awouters, H. 1967, "Pressure Dependence of the Viscosity of Liquid Argon and Liquid Oxygen, Measured by Means of a Torsionally Vibrating Quartz Crystal," Physica 34, 49-52.

Diller, D. E. 1980, "Measurements of the Viscosity of Compressed Gaseous and Liquid Methane," Physica 104A, 417-426.

Doscher, T. M. and El-Arabi, M. A. 1981, "High Pressure Model Studies of Oil Recovery by Carbon Dioxide," SPE 9787, presented at 1981 SPE/DOE Second Joint Symposium on Enhanced Oil Recovery, Tulsa, April 5-8.

Doscher, T. M., Oyekan, R., and El-Arabi, M. A. 1983, "A Controversial Laboratory Study of the Mechanism of Crude Oil Displacement by Carbon Dioxide: Part III-Nitrogen vs. Carbon Dioxide in Dipping Models," SPE 11678, presented at 53rd Annual California Regional Meeting, Ventura, March 23-25.

Dumoré, J. M. 1964, "Stability Considerations in Downward Miscible Displacements," Soc. Pet. Eng. J. 4, 356-362.

Ely, J. F. and Hanley H. J. M. 1981, "A Computer Program for the Prediction of Viscosity and Thermal Conductivity in Hydrocarbon Mixtures," U.S. National Bureau of Standards Tech. Note 1039.

Fussell, D. D. and Yanosik, J. L. 1978, "An Iterative Sequence for Phase Equilibria Calculations Incorporating the Redlich-Kwong Equation of State," Soc. Pet. Eng. J. 18, 173-182.

Fussell, L. T. 1979, "A Technique for Calculating Multiphase Equilibria," Soc. Pet. Eng. J. 19, 203-208.

Fussell, L. T. and Fussell, D. D. 1977, "An Iterative Technique for Compositional Reservoir Models," Soc. Pet. Eng. J. 19, 211-220.

Gardner, J. W., Orr, F. M., Jr., and Patel, P. D. 1981, "The Effect of Phase Behavior on CO_2 Flood Displacement Efficiency," J. Pet. Tech. 33, 2067-2081.

Gardner, J. W. and Ypma, J. G. J. 1982, "An Investigation of Phase Behavior-Macroscopic Bypassing in CO_2 Flooding," SPE 10686, presented at SPE/DOE Third Joint Symposium on Enhanced Oil Recovery, Tulsa, April 4-7.

Gelhar, L. W., Gutjahr, A. L., and Naff, R. L. 1979, "Stochastic Analysis of Macrodispersion in a Stratified Aquifer," Water Resources Research 15, No. 6, 1387-1397.

Haines, W. B. 1930, "Studies in the Physical Properties of Soils. V. The Hysteresis Effect in Capillary Properties and the Modes of Moisture Distribution Associated Therewith," J. Agric. Sci. 20, 97-116.

Haynes, W. M. 1973, "Viscosity of Gaseous and Liquid Argon," Physica 67, 440-470.

Helfferich, F. G. 1981, "Theory of Multicomponent, Multi-Phase Displacement in Porous Media," Soc. Pet. Eng. J. 21, 51-62.

Heller, J. P. 1966, "Onset of Instability Patterns Between Miscible Fluids in Porous Media," J. Appl. Phys. 37, 1566-1579.

Heller, J. P. 1963, "The Interpretation of Model Experiments for the Displacement of Fluids Through Porous Media," AIChE J. 9, 452-459.

Henry, R. L. and Metcalfe, R. S. 1980, "Multiple Phase Generation During CO_2 Flooding," SPE 8812, presented at First SPE/DOE Symposium on Enhanced Oil Recovery, Tulsa, April 20-23.

Holm, L. W. and Josendal, V. A. 1982, "Effect of Oil Composition on Miscible-Type Displacement by Carbon Dioxide," Soc. Pet. Eng. J. 22, 87-98.

Hunt, J. M. 1979, Petroleum Geochemistry and Geology, W.H. Freeman and Co., San Francisco.

Hutchinson, C. A., Jr. and Braun, P. H. 1961, "Phase Relations of Miscible Displacement and Oil Recovery," AIChE J. 7, 64-72.

Hutter, C. E., Franklin, J. C., Pelletier, M. T., Silva, M. K., and Orr, F. M., Jr. 1984, "Operation and Control of the Continuous Multiple Contact Experiment by the HP87XM Microcomputer," PRRC Report 84-7, Petroleum Recovery Research Center.

Jensen, C. M. and Orr, F. M., Jr. 1982a, "Phase Behavior of Mixtures of CO_2 and Wasson Crude Oil at 90°F, 105°F, and 120°F," PRRC Report 82-40, Petroleum Recovery Research Center (July).

Jensen, C. M. and Orr, F. M., Jr. 1982b, "Phase Behavior of Mixtures of CO_2 and Wasson Recombined Reservoir Fluid (312 SCF/BBL) at 90, 105 & 120°F," PRRC Report 82-41, Petroleum Recovery Research Center (July).

Jensen, C. M. and Orr, F. M., Jr. 1982c, "Phase Behavior of Mixtures of CO_2 and Wasson Recombined Reservoir Fluid (602 SCF/BBL) at 90, 105 & 120°F," PRRC Report 82-42, Petroleum Recovery Research Center (July).

Johnson, J. P. and Pollin, J. S. 1981, "Measurement and Correlation of CO_2 Miscibility Pressures," SPE 9790, presented at SPE/DOE Symposium on Enhanced Oil Recovery, Tulsa, April 5-8.

Kazemi, H., Vestal, C. R., and Shank, G. D. 1978, "An Efficient Multicomponent Numerical Simulator," Soc. Pet. Eng. J. 18, 355-368.

Kuan, D., Kilpatrick, P. K., Sahimi, M., Scriven, L. E., and Davis, H. T. 1983, "Multicomponent CO_2-Water-Hydrocarbon Phase Behavior Modelling: A Comparative Study," SPE 11961, presented at 58th Annual Technical Conference and Exhibition, San Francisco, October 5-9.

Lange, N. A. 1979, Lange's Handbook of Chemistry, John A. Dean Editor, Twelfth Edition, McGraw-Hill Book Company, New York.

Lantz, R. B. 1971, "Quantitative Evaluation of Numerical Diffusion (Truncation Error)," Soc. Pet. Eng. J. (September) 315.

Mason, G. and Morrow, N. R. 1983, "Meniscus Curvatures in Capillaries of Uniform Cross Section," submitted for publication.

Mason, W. P. 1947, "Measurement of the Viscosity and Shear Elasticity of Liquids by Means of a Torsionally Vibrating Crystal," Trans. A.S.M.E. (May) 359-370.

McCain, W. D., Jr. 1973, The Properties of Petroleum Fluids, Petroleum Publishing Company, Tulsa, Oklahoma.

McDonald, R. C. 1971, "Numerical Simulation with Interphase Mass Transfer," Report No. U7-71-a, Texas Petroleum Research Committee, Austin.

Mehra, R. K., Heidemann, R. A., and Aziz, K. 1982, "Computation of Multiphase Equilibrium for Compositional Simulation," Soc. Pet. Eng. J. 22, 61-68.

Meldrum, A. H. and Nielsen, R. F. 1955, "A Study of Three-Phase Equilibria for Carbon Dioxide-Hydrocarbon Mixtures," Prod. Monthly (August) 22-35.

Metcalfe, R. S. 1982, "Effects of Impurities on Minimum Miscibility Pressures and Minimum Enrichment Levels for CO_2 and Rich Gas Displacements," Soc. Pet. Eng. J. 22, 219-224.

Metcalfe, R. S. and Yarborough, L. 1979, "The Effect of Phase Equilibria on the CO_2 Displacement Mechanism," Soc. Pet. Eng. J. 19, 242-252.

Michels, A., Botzen, A., and Schuurman, W. 1957, "The Viscosity of Carbon Dioxide Between 0°C and 75°C at Pressures up to 2000 Atmospheres," Physica 23, 95-102.

Naar, J., Wygal, R. J., and Henderson, J. H. 1962, "Imbibition Relative Permeability in Unconsolidated Porous Media," Soc. Pet. Eng. J. 2, 13-17.

Newitt, D. M., Pai, M. U., Kuloor, N. R., and Huggill, J. A. 1956, "Carbon Dioxide" in Thermodynamic Functions of Gases, Vol. 1., F. Din, Ed., Butterworths, London, 102-134.

Nolen, J. S. 1973, "Numerical Simulation of Compositional Phenomena in Petroleum Reservoirs," SPE 4274, presented at SPE Third Symposium on Numerical Simulation, Houston, January 11-12.

Orr, F. M., Jr. 1980, "Simulation of One-Dimensional Convection of Four Phase, Four Component Mixtures," Topical Report DOE/ET/12082-8, U.S. Department of Energy, Bartlesville, Oklahoma.

Orr, F. M., Jr. and Jensen, C. M. 1984, "Interpretation of Pressure-Composition Phase Diagrams for CO_2-Crude Oil Systems," accepted Soc. Pet. Eng. J. (October).

Orr, F. M., Jr., Jensen, C. M., and Silva, M. K. 1981, "Effect of Solution Gas on the Phase Behavior of CO_2-Crude Oil Mixtures," presented at the International Energy Agency Workshop on Enhanced Oil Recovery, Winfrith, U.K., September 24.

Orr, F. M., Jr., Lien, C. L., and Pelletier, M. T. 1981, "Liquid-Liquid Phase Behavior in CO_2-Hydrocarbon Systems," Symposium on Chemistry of Enhanced Oil Recovery, American Chemical Society, Atlanta, March 29-April 3.

Orr, F. M., Jr. and Silva, M. K. 1983, "Equilibrium Phase Compositions of CO_2-Hydrocarbon Mixtures - Part 1: Measurement by a Continuous Multiple Contact Experiment," Soc. Pet. Eng. J. 23, 272-280.

Orr, F. M., Jr., Silva, M. K., and Lien, C. L. 1983, "Equilibrium Phase Compositions of CO_2-Crude Oil Mixtures - Part 2: Comparison of Continuous Multiple Contact and Slim Tube Displacement Tests," Soc. Pet. Eng. J. 23, 281-291.

Orr, F. M., Jr., Silva, M. K., Lien, C. L., and Pelletier, M. T. 1982, "Laboratory Experiments to Evaluate Field Prospects for CO_2 Flooding," J. Pet. Tech. 34, 888-898.

Orr, F. M., Jr. and Taber, J. J. 1983, "Displacement of Oil by Carbon Dioxide," Annual Report to the U.S. Department of Energy, Report No. DOE/BC/10331-9 (June).

Orr, F. M., Jr. and Taber, J. J. 1982, "Displacement of Oil by Carbon Dioxide," Annual Report to the U.S. Department of Energy, Report No. DOE/BC/10331-4 (April).

Orr, F. M., Jr. and Taber, J. J. 1981, "Displacement of Oil by Carbon Dioxide," Final Report to the U.S. Department of Energy, Report No. DOE/ET/12082-9 (May).

Orr, F. M., Jr., Yu, A. D., and Lien, C. L. 1981, "Phase Behavior of CO_2 and Crude Oil in Low Temperature Reservoirs," Soc. Pet. Eng. J. 21, 480-492.

Peng, D-Y and Robinson, D. B. 1976, "A New Two-Constant Equation of State," Ind. Eng. Chem. 15, No. 1, 59-64.

Perkins, T. K. and Johnston, O. C. 1963, " A Review of Diffusion and Dispersion in Porous Media," Soc. Pet. Eng. J. 3, 70-75.

Pope, G. A. and Nelson, R. C. 1978, "A Chemical Flooding Compositional Simulator," Soc. Pet. Eng. J. 18, 339-354.

Powell, M. J. D. 1964, "An Efficient Method for Finding the Minimum of a Function of Several Variables Without Calculating Derivatives," Computer J. 7, 155-162.

Raimondi, P. and Torcaso, M. A. 1964, "Distribution of the Oil Phase Obtained Upon Imbibition of Water," Soc. Pet. Eng. J. 4, 49-55.

Raimondi, P., Torcaso, M. A., and Henderson, J. H. 1961, "The Effect of Interstitial Water on the Mixing of Hydrocarbons during a Miscible Displacement Process," Mineral Industries Experimental Station Circular No. 61, The Pennsylvania State U., University Park (October 23-25).

Reamer, H. H., Fiskin, J. M., and Sage, B. H. 1951, "Phase Equilibria in Hydrocarbon Systems. Phase Behavior in the Methane-n-Butane-Decane System at 160°F," Ind. Eng. Chem. 41, 8871-8875.

Reamer, H. H. and Sage, B. H. 1963, "Phase Equilibria in Hydrocarbon Systems. Volumetric and Phase Behavior of the n-Decane-CO_2 System," J. Chem. Eng. Data 8, No. 4, 508-513.

Rossini, F. D. 1960, "Hydrocarbons in Petroleum," J. Chem. Education 37, No. 11, 554-561.

Ruschak, K. J. and Miller, C. A. 1972, "Spontaneous Emulsification in Ternary Systems with Mass Transfer," Ind. Eng. Chem. Fund. 11, No. 4, 534-540.

Saffman, P. G. and Taylor, G. I. 1958, "The Penetration of a Fluid into a Porous Medium or Hele-Shaw Cell Containing a More Viscous Liquid," Proc. Royal Soc., London 245, 312.

Sage, B. H. and Lacey, W. N. 1955, Some Properties of the Lighter Hydrocarbons, Hydrogen Sulfide, and Carbon Dioxide, American Petroleum Institute.

Salter, S. J. and Mohanty, K. K. 1982, "Multiphase Flow in Porous Media: I. Macroscopic Observations and Modelling," SPE 11017, presented at 57th Annual Fall Technical Conference and Exhibition, New Orleans, September 26-29.

Schneider, G. 1968, "Phase Equilibria in Binary Fluid Systems of Hydrocarbons with Carbon Dioxide, Water and Methane," AIChE Symposium Series, 64, 9-15.

Schneider, G., Alwani, Z., Heim, W., Horvath, E., and Franck, E. U. 1967, "Phasengleichgewichte und kritische Erscheinungen in binaren Michsystemen bis 1500 bar: CO_2 mit n-Octan, n-Undecan, n-Tridecan und n-Hexadecan," Chem. Ing. Tech. 39, 649-656.

Scott, R. L. and van Konynenburg, P. H. 1970, "Static Properties of Solutions," Disc. Faraday Soc. 49, 87-97.

Shelton, J. L. and Schneider, F. N. 1975, "The Effects of Water Injection on Miscible Flooding Methods Using Hydrocarbons and Carbon Dioxide," Soc. Pet. Eng. J. 15, 217-226.

Sigmund, P. M., Aziz, K., Lee, J. J., Nghiem, L. X., and Mehra, R. 1979, "Laboratory CO_2 Floods and Their Computer Simulation," World Petroleum Congress, Bucharest, Romania, September.

Silva, M. K., Larsen, L. L., Lien, C. L., and Orr, F. M., Jr. 1983, "Measured Phase Compositions and Densities for CO_2-C_1-C_4-C_{10} Systems at 160°F and 1250 psia and Phase Compositions and Densities by Peng-Robinson EOS for Systems at 160°F and Pressures from 750 to 2250 psia," PRRC Report 83-24, Petroleum Recovery Research Center (December).

Silva, M. K., Lien, C. L., Franklin, J. C., and Orr, F. M., Jr. 1982a, "Phase Compositions and Densities of Mixtures of CO_2 with Rock Creek Separator Oil with Aromatic Spikes at 75°F and 1300 psia," PRRC Report 82-27, Petroleum Recovery Research Center (June).

Silva, M. K., Lien, C. L., Franklin, J. C., and Orr, F. M., Jr. 1982b, "Phase Compositions and Densities of Mixtures of CO_2 with Maljamar Separator Oil at 90°F and 1000 psia," PRRC Report 82-5, Petroleum Recovery Research Center (January).

Silva, M. K., Lien, C. L., Franklin, J. C., and Orr, F. M., Jr. 1981a, "Phase Compositions and Densities of Mixtures of CO_2 with Maljamar Separator Oil at 90°F and 1400 psia," PRRC Report 81-51, Petroleum Recovery Research Center (November).

Silva, M. K., Lien, C. L., Franklin, J. C., and Orr, F. M., Jr. 1981b, "Phase Compositions and Densities of Mixtures of CO_2 with Maljamar Separator Oil at 90°F and 1200 psia," PRRC Report 81-53, Petroleum Recovery Research Center (November).

Silva, M. K., Lien, C. L., Pelletier, M. T., and Orr, F. M., Jr. 1981c, "Phase Compositions for Mixtures of CO_2 with Maljamar Separator Oil at 90°F and 800 psia," PRRC Report 81-30, Petroleum Recovery Research Center (July).

Simon, R. and Schmidt, R. L. 1983, "A System for Determining Fluid Properties Up to 136 MPa and 473 K," Proceedings, Symposium on Supercritical Fluids: Their Chemistry and Application, Faraday Division, Roy. Soc. Chem., Cambridge, England (September) Elsevier.

Spence, A. P. and Watkins, R. W. 1980, "The Effect of Microscopic Core Heterogeneity on Miscible Flood Residual Oil Saturation," SPE 9229, presented at 55th Annual Fall Meeting of SPE of AIME, Dallas, September 21-24.

Stalkup, F. I., Jr. 1983, Miscible Displacement, Monograph Volume 8, Society of Petroleum Engineers of AIME, New York.

Stalkup, F. I. 1970, "Displacement of Oil by Solvent at High Water Saturation," Soc. Pet. Eng. J. 10, 337-348.

Stewart, W. C. and Nielson, R. F. 1954, "Phase Equilibria for Mixtures of Carbon Dioxide and Several Normal Saturated Hydrocarbons," Prod. Monthly (January) 27-32.

Taylor, G. I. 1953, "Dispersion of Soluble Matter in Solvent Flowing Slowly Through a Tube," Proc., Royal Soc. 219, London, 186-203.

Taylor, M. A. 1984, "Effects of 10% N_2 Contamination in CO_2 on the Phase Behavior of Wasson Crude Oil-CO_2 Mixtures," PRRC Report 84-6, Petroleum Recovery Research Center.

Thomas, G. H., Countryman, G. R., and Fatt, I. R. 1963, "Miscible Displacement in a Multiphase System," Soc. Pet. Eng. J. 3, 189-196.

Tiffin, D. L. and Yellig, W. F. 1983, "Effects of Mobile Water on Multiple Contact Miscible Gas Displacements," Soc. Pet. Eng. J. 23, 447-455.

Todd, M. R. 1979, "Modeling Requirements for Numerical Simulation of CO_2 Recovery Processes," SPE 7998, presented at the California Regional Meeting of SPE, Ventura, April 18-20.

Todd, M. R. and Longstaff, W. J. 1972, "The Development, Testing and Application of a Numerical Simulator for Predicting Miscible Flood Performance," J. Pet. Tech. 24, 874-882.

Wang, G. C. 1982, "Microscopic Investigation of CO_2 Flooding Process," J. Pet. Tech. 34, 1789-1797.

Wang, G. C. 1980, "Microscopic Study of Oil Recovery by Carbon Dioxide," Final Report DOE/MC/12095-7 (December).

Wardlaw, N. C. 1980, "The Effects of Pore Structure on Displacement Efficiency in Reservoir Rocks and in Glass Micromodels," SPE 8843, presented at First SPE/DOE Symposium on Enhanced Oil Recovery, Tulsa, April 20-23.

Wardlaw, N. C. and Cassan, J. P. 1978, "Estimation of Recovery Efficiency by Visual Observation of Pore Systems in Reservoir Rocks," Can. Pet. Geol. Bull. 26, No. 4, 572.

Watkins, R. W. 1978, "A Technique for the Laboratory Measurement of Carbon Dioxide Unit Displacement Efficiency in Reservoir Rock," SPE 7474, presented at SPE 53rd Annual Fall Meeting, Houston, October 1-3.

Webeler, R. W. H. 1961, "Viscosity X Density Measurements for Normal Liquid Hydrogen and Various Ortho-Para Mixtures," Ph.D. Thesis, University of Cincinnati.

Welber, B. 1960, "Damping of a Torsionally Oscillating Cylinder in Liquid Helium at Various Temperatures and Densities," Physical Review 119, No. 6 (September) 1816-1822.

Yellig, W. F. 1982, "Carbon Dioxide Displacement of a West Texas Reservoir Oil," Soc. Pet. Eng. J. (December) 805-815.

Yellig, W. F. and Baker, L. E. 1980, "Factors Affecting Miscible Flooding Dispersion Coefficients," presented at the 31st Annual Technical Meeting of the Petroleum Society of CIM in Calgary, May 25-28.

Yellig, W. F. and Metcalfe, R. S. 1980, "Determination and Prediction of CO_2 Minimum Miscibility Pressures," J. Pet. Tech. 32, 160-168.

APPENDIX A

This section reports results of work on the experimental technique described previously for continuous measurement of phase compositions and fluid properties (Orr, Silva, Lien & Pelletier 1982; Orr & Taber 1982; Orr & Silva 1983; Orr, Silva & Lien 1983). Detailed documentation of the communication between the HP87XM microcomputer and experimental equipment is available (Hutter et al 1984).

Equipment Modifications

An experimental difficulty was encountered in an attempt to measure phase compositions when the two-phase region was entered through a dew point. In that case, circulation of fluid from the bottom to the top of the cell caused lower phase sample contamination problems, because there was an insufficient volume of lower phase available to satisfy the holdup in the circulation system. To alleviate this problem, additional valves were added to the circulation loop to facilitate reversal of the direction of circulation. The revised system is shown in Fig. A.1. An additional umbrella was added to the lower sampling port to allow collection of samples from a quiescent zone when the circulation is from top to bottom. The new circulation system allows reversal of flow direction during an experiment. Thus, when a two-phase region has been entered through a bubble point, and progresses to the point where the remaining lower phase volume is too small to permit sampling from the bottom of the cell, the direction of flow can be reversed, and the collection of clean samples through the multiphase region can continue; therefore, a wider range of compositions can be investigated.

While the alterations to the circulation system were minor, much more extensive modifications have been made to the equipment which controls the experiment and records data during the run. The experiment is now controlled by an HP87XM microcomputer which:

- Reads densitometer output; calculates and stores upper and lower phase densities.
- Advances multiport samplers at the end of a sample period; alternates back pressure regulators between the upper and lower phases.
- Selects appropriate (upper or lower) sample streams and sets the position of a sample switching valve in the gas chromatograph.
- Starts gas chromatograph analysis of gas samples.
- Reads and stores results of analysis.

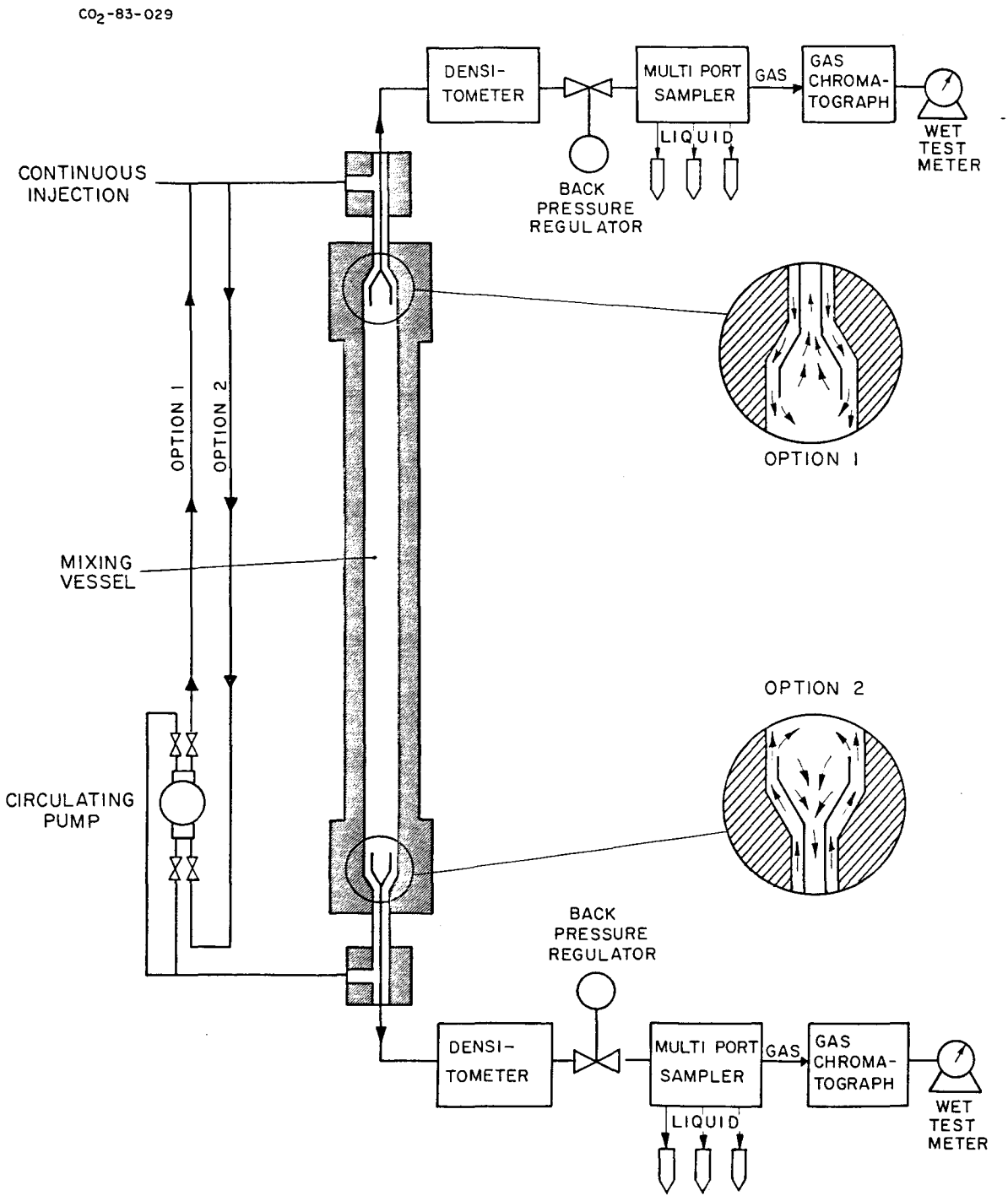

Fig. A.1 Continuous multiple contact apparatus.

The new system is quite flexible. It allows the operator to select the length of a sample collection period, to specify how rapidly the system switches back and forth between the upper and lower sample streams by selecting which back pressure regulator controls sample production, to set how often gas chromatograph (GC) produced gas samples are analyzed, and to specify how frequently phase density readings are taken. In addition, any of these parameters can be changed during a run if desired.

A schematic of the data communications system is shown in Fig. A.2. The control programs operate on a standard Hewlett-Packard HP87XM microcomputer to which a BCD interface (NP82941A), a serial interface (HP82939A) and an I/O ROM have been added. The BCD interface is used to receive data from the densitometers (Mettler/Paar DMA512) and to handle several switching and control functions. The interface has ten ports. Nine are standard data ports which can receive data from an instrument. The tenth is a special port (port 10) which can be used to transmit data to one or more instruments. The four digits available on the special port are used as follows:

Digit 1 (2^0) - Select upper or lower back pressure regulator.

Digit 2 (2^1) - Advance multiport sampling valves.

Digit 3 (2^2) - Start a GC run.

Digit 4 (2^3) - Switch the GC sample valve to the other sample stream.

When digit 1 is set high (1), the upper back pressure regulator controls the sample production rate. When it is low (0), the lower regulator controls. To advance the multiport sampling valves which are used to separate liquid and vapor downstream of the back pressure regulators, digit 1 is set high for approximately one second and then set low. To start a gas chromatograph run, digit 2 is set high for approximately one second and then set low. The sample valve in the gas chromatograph collects lower phase gas when digit 3 is set low. When it is set high, upper phase gas is sampled. The timing of these functions is set by the operator. Typical time settings are:

- Collect density data every 4 minutes.
- Alternate the back pressure regulators every 3 minutes.
- Start a GC run every 15 minutes.
- Advance to the next sample every hour.

The sample valve on the GC is always set to switch 6 seconds after the start of a GC run. At that point the sample in the sample loop has been injected on column and the sample valve is free to begin collecting the next sample.

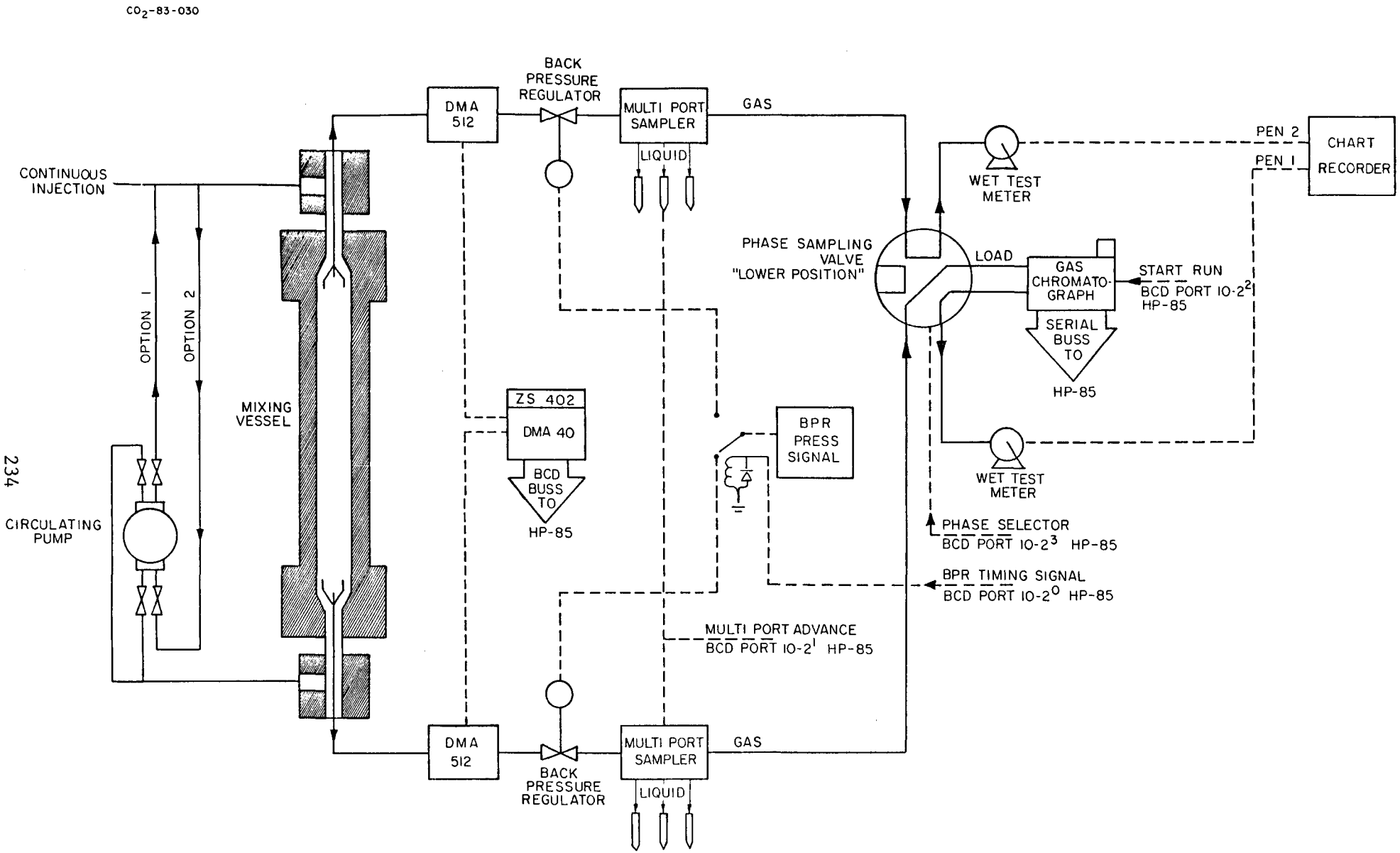

Fig. A.2 Flowchart of data communications system.